

Recent Progress in Radiative-Rate Determination of Some Heavy Ions (Xe^{9+} , Xe^{10+} , Lu^{3+} , Hf^{4+} , Ta^{5+}) of Interest in Fusion

Saturnin Enzonga Yoca^{1,2}

¹Faculty of Sciences and Techniques, Marien Ngouabi University, Brazzaville, Congo

²African and Malagasy Council for Higher Education—CAMES, Ouagadougou, Burkina Faso

Email: saturnin.enzongayoca@umng.cg

How to cite this paper: Yoca, S.E. (2021) Recent Progress in Radiative-Rate Determination of Some Heavy Ions (Xe^{9+} , Xe^{10+} , Lu^{3+} , Hf^{4+} , Ta^{5+}) of Interest in Fusion. *Journal of Applied Mathematics and Physics*, **9**, 2848-2888.

<https://doi.org/10.4236/jamp.2021.911182>

Received: October 15, 2021

Accepted: November 16, 2021

Published: November 19, 2021

Copyright © 2021 by author(s) and Scientific Research Publishing Inc.

This work is licensed under the Creative Commons Attribution International License (CC BY 4.0).

<http://creativecommons.org/licenses/by/4.0/>



Open Access

Abstract

This paper presents a review about the radiative properties (transition probabilities and oscillator strengths) of two xenon ions (Xe^{9+} , Xe^{10+}) and three members of Er I isoelectronic sequence (Lu^{3+} , Hf^{4+} , Ta^{5+}) of interest in controlled thermonuclear fusion, including our recent theoretical data obtained using two independent theoretical atomic structure computational approaches (semi-empirical Hartree-Fock with relativistic corrections method (HFR) and the *ab initio* multiconfiguration Dirac-Hartree-Fock (MCDHF)). The tables, from the second one, summarize the recommended data expected to be useful for plasma modelling in fusion.

Keywords

Atomic Spectra, Atomic Data, Transition Probabilities, Oscillator Strengths, Heavy Elements

1. Introduction

There is a growing need in atomic data for elements which could be used in thermonuclear fusion installations for the fuel introduction or as plasma facing materials. Noble gases can be injected into nuclear fusion reactors, conditioned in solid pellets, for both plasma diagnostics and fuel introduction [1] [2] [3]. In particular, if xenon ($Z = 54$) was inserted into the international thermonuclear experimental reactor (ITER) which will be the next step towards the realization of fusion, it could be pumped out without leaving residuals on plasma facing material and would therefore be recycled in subsequent discharges. Moreover, the xenon atoms would strip to helium-like ions in the hottest part of the confined plasma. Consequently, the identification of emission lines and the know-

ledge of spectroscopic parameters from all ionization stages of xenon, including Xe^{9+} and Xe^{10+} , would be of key importance in order to model the plasma and facilitate the analysis of the spectra used for the estimation of physical conditions inside the fusion reactors such as densities and temperatures.

Up to now, experimental and theoretical investigations on spectroscopic properties of xenon ions have been performed. Recently, a review by Almandos and Raineri [4] reported the extensive use of Pulsed discharges in La Plata (Argentina) to produce spectra of Xe III-IX falling in ultraviolet (UV), visible and infrared regions [5]-[11], so as to identify the corresponding lines. In those studies, time-resolved experiments and relativistic Hartree-Fock calculations were also carried out to obtain radiative lifetimes and transition probabilities. Biémont's team [12] [13] [14] [15] realized large-scale calculations of lifetimes, oscillator strengths and transition probabilities in moderately charged xenon ions (Xe V-Xe IX) by combining often theory (HFR/HFR+CPOL [16], MCDF [17] [18] [19] [20]) and experiment (Beam Foil Spectroscopy [21]). Saloman [22] compiled the energy levels and observed spectral lines of the xenon atom in all stages of ionization for which experimental data are available before 2004, *i.e.* Xe I-Xe XI, Xe XIX, Xe XXV-Xe XXIX, Xe XLIII-Xe XLV, and Xe LI-Xe LIV. In that compilation, data on Xe^{9+} and Xe^{10+} were respectively based on Refs. [23] [24] and [25]. It should be noted that in Refs. [24] [25] the authors reported some radiative parameters, including transition probabilities. From 2004, the main works on Xe^{9+} and Xe^{10+} are those of [26] [27] and [28] [29] [30], respectively. In Refs. [27] [30], as an extension of works by Biemont *et al.* [12] [13] [14] [15], we used two different theoretical approaches, *i.e.* the semi-empirical Hartree-Fock with relativistic corrections (HFR) and the fully relativistic multiconfiguration Dirac-Hartree-Fock (MCDHF) methods, to obtain two new sets of oscillator strengths and transition probabilities of radiative transitions in Xe^{9+} and Xe^{10+} , in the extreme ultraviolet region.

Lutetium ($Z = 71$), hafnium ($Z = 72$) and tantalum ($Z = 73$) would be candidates as plasma-facing materials in controlled nuclear fusion devices [31] [32] [33] [34]. In addition, the last two of them are also produced in neutron-induced transmutation of tungsten ($Z = 74$) and tungsten-alloys that will compose the divertors in future tokamaks [35]. As a result, their sputtering may generate ionic impurities of all possible charge states, including the members of Er I isoelectronic sequence (Lu IV, Hf V, Ta VI), in the deuterium-tritium plasma that could contribute to radiation losses in fusion reactors. Therefore, the radiative properties of these ions have potentially important applications in this field. Unfortunately, there are very few studies devoted to the transition rates of these ions. The only data available have been computed in the Er I isoelectronic sequence by Anisimova *et al.* [36] (Yb III, Lu IV, and Hf V), Loginov and Tuchkin [37] (Yb III, Lu IV, Hf V, and Ta VI) and Bokamba *et al.* [38] (Lu IV, Hf V, and Ta VI). In the two first Refs, the authors utilized the Newton and least-squares monoconfigurational methods without taking into account that an appropriate treatment of these ions must be done in the framework of the configuration in-

teraction. Recently, we reported in Ref. [38] extensive calculations of transition probabilities and oscillator strengths in Lu³⁺, Hf⁴⁺ and Ta⁵⁺ using the same methods as in the case of Xe⁹⁺ and Xe¹⁰⁺ [27] [30] that consider both the electron correlations and configuration interaction. The three new sets of obtained transition probabilities and oscillator strengths fall in the spectral domain from ultraviolet to infrared.

In this review, we briefly describe the methods used for obtaining the most recent radiative properties (transition probabilities and oscillator strengths) in Xe⁹⁺, Xe¹⁰⁺, Lu³⁺, Hf⁴⁺ and Ta⁵⁺, *i.e.* MCDHF and HFR (Section 2). Section 3 is devoted to the discussion of the available radiative transition rates in these ions, as well as the selection of data expected reliable. Finally, the concluding remarks are given in Section 4.

2. Theoretical Methods

Xe⁹⁺, Xe¹⁰⁺, Lu³⁺, Hf⁴⁺ and Ta⁵⁺ being heavy ions, it is therefore important to take into account both the configuration interaction (CI) and relativistic effects for modelling their atomic structure and computing radiative rates. In the most recent radiative-rate investigations of these ions [27] [30] [38], we utilized, in view of no radiative rate measurements available in the literature, two independent theoretical methods, *i.e.* the semi-empirical Hartree-Fock with relativistic corrections method (HFR) and the *ab initio* multiconfiguration Dirac-Hartree-Fock method (MCDHF), both of them including explicitly the most important intravalance and core-valence electron correlations. **Table 1** reports the HFR and MCDHF physical models used in Refs. [27] [30] [38].

Table 1. Physical models used in our work [27] [30] [38].

Ion	Physical models ^a	
	HFR	MCDHF ^c
Xe ⁹⁺	Even parity: <u>4d⁹</u> , 4d ⁸ s, 4d ⁸ s, 4d ⁸ 7s, 4d ⁸ 5d, 4d ⁸ 6d, 4d ⁷ 5s ² , 4d ⁷ 5p ² , 4d ⁷ 5d ² , 4d ⁷ 5s6s, 4d ⁷ 5s5d, 4d ⁷ 5s6d, 4p ⁵ 4d ⁹ 5p Odd parity: <u>4d⁸5p</u> , 4d ⁸ 6p, 4d ⁸ 7p, <u>4d⁸4f</u> , 4d ⁸ 5f, 4d ⁸ 6f, 4d ⁷ 5s5p, 4d ⁷ 5s6p, 4d ⁷ 5p5d, 4d ⁷ 5p6s, <u>4p⁵4d¹⁰</u>	4s, 4p, 4d, 4f, 5 s, 5p, 5d, 5f
Xe ¹⁰⁺	Even parity: <u>4d⁸</u> , 4d ⁷ ns (n = 5 - 7), 4d ⁷ nd (n = 5 - 6), 4d ⁶ 5s ² , 4d ⁶ 5p ² , 4d ⁶ 5d ² , 4d ⁶ 5s6s, 4d ⁶ 5s5d, 4p ⁵ 4d ⁸ 5p Odd parity: <u>4d⁷5p</u> , 4d ⁷ np (n = 6 - 7), <u>4d⁷4f</u> , 4d ⁷ nf (n = 5 - 6), 4d ⁶ 5snp (n = 5 - 6), 4d ⁶ 5p5d, <u>4p⁵4d⁹</u>	4p, 4d, 4f, 5 s, 5p, 5d, 5f
Lu ³⁺ , Hf ⁴⁺	Even parity: <u>4f¹⁴</u> , <u>4f¹³6p</u> , 4f ¹³ 7p, <u>4f¹³5f</u> , 4f ¹³ nf (n = 6 - 7), 4f ¹² 5d ² , 4f ¹² 6s ² , 4f ¹² 6p ² , 4f ¹² 5d6s, 5p ⁵ 6p ^b	4f, 5p, 5d, 5f, 6s, 6p
Ta ⁵⁺	Odd parity: <u>4f¹³5d</u> , <u>4f¹³6d</u> , 4f ¹³ 7d, <u>4f¹³6s</u> , 4f ¹³ 7s, 4f ¹² 5d6p, 4f ¹² 6s6p, 5p ⁵ 4f ¹⁴ 5d ^b , 5p ⁵ 4f ¹⁴ 6s ^b	6d, 6f, 7s, 7p, 7d, 7f

a: Underlined configurations are spectroscopic ones, used as reference configurations in MCDHF. b: spectroscopic configurations in Ta⁵⁺ in addition to the ones in Lu³⁺ and Hf⁴⁺. c: Active set of orbitals to which there are single and double electron excitations in MCDHF.

2.1. Multiconfiguration Dirac-Hartree-Fock Method

In the multiconfiguration Dirac-Hartree-Fock (MCDHF) method implemented in the GRASP2K and GRASP2018 computer packages [39] [40], the Hamiltonian is given by

$$H = \sum_i^N \left(c\alpha_i \cdot p_i + (\beta_i - 1)c^2 + \frac{Z}{r_i} \right) + \sum_{i < j}^N \frac{1}{r_{ij}}, \quad (1)$$

where c is the speed of light, α and β are the Dirac matrices.

The atomic state function (ASF), Ψ , is represented by a superposition of configuration state functions (CSF), Φ , with the same parity, π , total angular momentum and total magnetic quantum numbers, J and M_J , forming a basis set of the representation, $\{\Phi_k\}$, as

$$\Psi(\Pi JM_J) = \sum_k c_k \Phi(\gamma_k \Pi JM_J), \quad (2)$$

where c_k are the mixing coefficients, γ_k represent all the other quantum numbers needed to uniquely specify CSF that are jj -coupled Slater determinants built from one-electron spin-orbitals, $\phi_{nkm}(r, \theta, \varphi)$, of the form:

$$\phi_{nkm}(r, \theta, \varphi) = \frac{1}{r} \begin{pmatrix} P_{nk}(r) \chi_{km}(\theta, \varphi) \\ iQ_{nk}(r) \chi_{km}(\theta, \varphi) \end{pmatrix} \quad (3)$$

$P_{nk}(r)$ and $Q_{nk}(r)$ are, respectively, the large and the small radial components of the wave functions, and the angular functions $\chi_{km}(\theta, \varphi)$ are the spinor spherical harmonics [39]. The quantum number κ is given by:

$$\kappa = \pm \left(j + \frac{1}{2} \right) = a \left(j + \frac{1}{2} \right) \quad (4)$$

so that

$$l = j - \frac{1}{2}a \quad (5)$$

The radial functions $P_{nk}(r)$ and $Q_{nk}(r)$ are numerically represented on a logarithmic grid and are required to be orthonormal within each κ symmetry. In the MCDHF variational procedure, the radial functions and the expansion coefficients c_k are optimized to self-consistency [39] [41], which can be done employing different options:

- Average Level calculation (AL), spin-orbitals are chosen to minimize the average energy of configuration state functions with different total angular momentum J ;
- Optimal Level calculation (OL), only the energy of an individual level is minimized;
- Extended Optimal Level calculation (EOL), the minimization is extended over several selected levels;
- Extended Average Level calculation (EAL), averaging of the energy expression is extended to all configuration functions, usually using statistical weights $(2J + 1)$ as weighting factors.

In the Relativistic Configuration Interaction (RCI) step, the eigenvalue problem is solved in a CSF basis built with a fixed preoptimized orbital set [42].

The relativistic two-body Breit interaction and the quantum electrodynamic corrections due to self-energy and vacuum polarization are also considered through the implementation of the routines developed by McKenzie *et al.* [19].

The final transition amplitudes are computed in both the Babushkin (B) and the Coulomb (C) gauges which are respectively the relativistic equivalents of the length and velocity gauges. The gauges agreement for a given transition, *i.e.* $0.9 \leq B/C \leq 1.1$, provides an indication of the accuracy of its transition probability although this condition is necessary but not sufficient [43]. Cowan proposed an independent accuracy indicator, *i.e.* the cancellation factor (CF), defined for the E1 transitions as below [44]:

$$CF = \left(\frac{\left| \sum_k \sum_i c_k \langle \Phi'(\gamma_k \Pi' J' M_{J'}) | P^{(1)} | \Phi(\gamma_i \Pi J M_J) \rangle c_i \right|^2}{\sum_k \sum_i \left| \langle \Phi'(\gamma_k \Pi' J' M_{J'}) | P^{(1)} | \Phi(\gamma_i \Pi J M_J) \rangle c_i \right|^2} \right)^{1/2} \quad (6)$$

where $P^{(1)}$ is the electric dipole operator and $c_{i(k)}(')$ and $\Phi_{i(k)}(')$ have the same meanings as in Equation (2) for the initial (non-primed symbols) and final (primed symbols) states of the transition. Computed line strength with a small value of the CF, *e.g.* less than 0.05, is strongly affected by destructive interference effects resulting from intermediate-coupling and interaction-configuration mixing of basis states. The GRASP2K and GRASP2018 packages have been modified in order to implement the calculation of this latter accuracy indicator [38] [43]. Computed line strength may thus be expected reliable if it simultaneously fulfills these conditions [43]:

$$0.90 \leq B/C \leq 1.10 \text{ and } CF \geq 0.05 \quad (7)$$

2.2. Relativistic Hartree-Fock Method

In the Hartree-Fock method with relativistic corrections (HFR) of Cowan [44], a set of orbitals is obtained for each electronic configuration by solving the Hartree-Fock equations for the spherically averaged atom. The equations resulting from the application of the variational principle to the configuration average energy. Relativistic corrections are included in this set of equations, *i.e.* the Blume-Watson spin-orbit, mass-velocity and one-body Darwin terms. The Blume-Watson spin-orbit term comprises the part of the Breit interaction that can be reduced to a one-body operator.

The multiconfiguration Hamiltonian matrix is constructed and diagonalized in the $LSJM_J\pi$ representation within the framework of the Slater-Condon theory [45]. Each matrix element is a sum of products of Racah angular coefficients and radial integrals, *i.e.*

$$H_{ab} = \langle \alpha_a L_a S_a JM_J \pi | H | \alpha_b L_b S_b JM_J \pi \rangle = \sum_i c_i^{a,b} I_i^{a,b}, \quad (8)$$

where $c_i^{a,b}$ and $I_i^{a,b}$ stand for the angular coefficients and the radial parame-

ters, respectively. The radial parameters correspond to the configuration average energies (E_{av}), the mono-configuration (P^k , G^k) and configuration interaction (R^k) Slater integrals, the spin-orbit parameters (ζ_{nl}) and, if necessary, the effective interaction parameters (α , β , γ) [44]. These parameters can be adjusted to fit the eigenvalues of the Hamiltonian to the available observed energy levels in a least-squares approach. Note that this approach is linked more strongly to the quantity and the quality of the experimental energy levels. The eigenvalues and the eigenstates resulting from this way (*ab initio* or semi-empirically) are used to compute the wavelength, the transition probability and the oscillator strength for each possible transition. Concerning an allowed line (E1), the cancellation factor (CF) as described in Equation (6) constitutes a reliable indicator for its computed line strength.

3. Radiative Transitions

3.1. Xenon ions, Xe^{9+} and Xe^{10+}

3.1.1. Ion Xe^{9+}

Wavelengths of the observed lines and energy levels in the Xe X spectrum were compiled by Saloman [22] who critically evaluated the previous data published by Kaufman *et al.* [23] and Churilov and Joshi [24].

Churilov and Joshi [24], in their spectral analysis of Xe X, were helped by the computed transition probabilities obtained by HFR method using Cowan codes [44], and those data were the first in the literature. Fahy *et al.* [26] observed Xe^{9+} lines in the 140 - 150 Å range employing an electron beam ion trap and a flat field spectrometer, and they reported seven strongest lines along with their HFR gA-values. More recently, we used two independent theoretical approaches HFR and MCDHF to obtain a set of radiative properties (oscillator strengths and transition probabilities) for 92 Xe X allowed spectral lines belonging to the $4d^9 - (4d^85p + 4d^84f + 4p^54d^{10})$ transition arrays, for which $\log gf > -4$, falling in the extreme ultraviolet (EUV) range 100 - 164 Å [27]. Half of those E1 transitions meet the adopted reliability criteria (7).

When comparing the expected reliable data from our two computational methods satisfying the accuracy criteria (7) [27], we have found the average ratio $\langle gA_{\text{MCDHF}}/gA_{\text{HFR}} \rangle \sim 1.05 \pm 0.60$, showing thus a good overall agreement between the two approaches.

The weighted transition probabilities by Churilov and Joshi [24] are compared with our MCDHF and HFR values satisfying the adopted reliability criteria (7), the average rates are respectively $\langle gA(\text{MCDHF})/gA([24]) \rangle = 1.14 \pm 0.77$ and $\langle gA(\text{HFR})/gA([24]) \rangle = 1.08 \pm 0.13$. The MCDHF calculations include more correlation than HFR technique by Churilov and Joshi [24], which could explain the difference observed between the two sets of results. As for the about 8% overall discrepancy between our HFR values with the data by Churilov and Joshi [24] obtained with a similar HFR approach [24], the authors' restricted physical model is certainly the possible explanation. In addition, the main purpose of

these researchers was the term analysis of the Xe^{9+} ion. In this work, we have adopted the MCDHF transition probabilities reported by Bokamba *et al.* [27].

We report in **Table 2** the adopted transition probabilities (column 3), and column 4 contains other available data.

Table 2. Adopted transition probabilities (gA) in Xe X, as well as other available gA-values.

λ (nm) ^a	Transition	Adopted gA (s^{-1}) ^b	Other gA (s^{-1})
11.0133	$16,725_{3/2} - 924,721_{1/2}^o$	3.10E+12	3.84E+12 ^c , 3.80E+12 ^d
11.2714	$0_{5/2} - 887,203_{5/2}^o$	3.68E+10	1.03E+11 ^c , 9.70E+10 ^d , 1.20E+11 ^e
11.3438	$0_{5/2} - 881,539_{3/2}^o$	5.96E+11	2.28E+12 ^c , 2.26E+12 ^d , 4.41E+12 ^e
114.313	$0_{5/2} - 874,794_{3/2}^o$	5.48E+12	5.02E+12 ^c , 4.94E+12 ^d , 2.95E+12 ^e
11.4879	$16,725_{3/2} - 887,203_{5/2}^o$	9.24E+12	1.08E+13 ^c , 1.07E+13 ^d , 1.07E+13 ^e
11.4880	$0_{5/2} - 870,470_{7/2}^o$	1.24E+13	1.47E+13 ^c , 1.44E+13 ^d , 1.45E+13 ^e
11.5632	$16,725_{3/2} - 881,539_{3/2}^o$	5.32E+12	4.76E+12 ^c , 4.68E+12 ^d , 2.88E+12 ^e
11.5661	$0_{5/2} - 864,592_{5/2}^o$	8.76E+12	9.98E+12 ^c , 9.80E+12 ^d , 9.82E+12 ^e
13.5729	$16,725_{3/2} - 753,489_{1/2}^o$	5.20E+10	6.78E+10 ^c , 6.20E+10 ^d
14.1545	$16,725_{3/2} - 723,216_{1/2}^o$	1.76E+10	1.27E+10 ^c , 1.10E+10 ^d
14.2046	$0_{5/2} - 703,997_{7/2}^o$	4.52E+10	4.11E+10 ^c , 4.20E+10 ^d
14.3477	$0_{5/2} - 696,975_{3/2}^o$	2.15E+10	1.98E+10 ^c , 1.40E+10 ^d
14.4654	$0_{5/2} - 691,306_{3/2}^o$	5.80E+10	3.04E+10 ^c , 2.50E+10 ^d
14.4769	$0_{5/2} - 690,757_{5/2}^o$	2.47E+10	1.38E+10 ^c , 1.40E+10 ^d
14.5150	$16,725_{3/2} - 705,669_{1/2}^o$	2.00E+11	2.07E+11 ^c , 2.01E+11 ^d
14.5323	$0_{5/2} - 688,121_{3/2}^o$	1.02E+11	9.35E+10 ^c , 9.40E+10 ^d
14.5983	$16,725_{3/2} - 701,735_{5/2}^o$	2.65E+11	1.89E+11 ^c , 1.81E+11 ^d
14.6148	$0_{5/2} - 684,240_{7/2}^o$	2.82E+10	1.13E+10 ^c , 1.00E+10 ^d
14.6413	$0_{5/2} - 682,998_{3/2}^o$	3.89E+10	4.01E+10 ^c , 2.40E+10 ^d
14.6448	$0_{5/2} - 682,838_{5/2}^o$	5.03E+09	1.46E+10 ^c , 1.30E+10 ^d
14.7381	$16,725_{3/2} - 695,239_{1/2}^o$	1.98E+10	1.82E+10 ^c , 1.90E+10 ^d
14.7619	$0_{5/2} - 677,421_{3/2}^o$	2.68E+11	2.37E+11 ^c , 2.26E+11 ^d
14.7638	$16,725_{3/2} - 694,056_{5/2}^o$	5.58E+10	6.56E+10 ^c , 6.60E+10 ^d
14.7956	$0_{5/2} - 675,878_{7/2}^o$	4.19E+11	3.45E+11 ^c , 3.21E+11 ^d
14.8005	$0_{5/2} - 675,652_{5/2}^o$	2.33E+11	1.53E+11 ^c
14.8240	$16,725_{3/2} - 691,306_{3/2}^o$	7.92E+10	2.08E+10 ^c , 1.60E+10 ^d
14.8333	$0_{5/2} - 674,159_{3/2}^o$	7.60E+09	4.95E+10 ^c , 5.20E+10 ^d
14.8361	$16,725_{3/2} - 690,757_{5/2}^o$	1.16E+11	1.31E+11 ^c , 1.29E+11 ^d
14.8707	$16,725_{3/2} - 689,190_{3/2}^o$	1.99E+06	4.65E+10 ^c , 4.80E+10 ^d
14.8943	$16,725_{3/2} - 688,121_{3/2}^o$	1.41E+11	1.47E+11 ^c , 1.33E+11 ^d
14.9021	$0_{5/2} - 671,045_{5/2}^o$	1.82E+11	1.47E+11 ^c , 1.33E+11 ^d
14.9358	$0_{5/2} - 669,531_{7/2}^o$	1.13E+11	1.93E+11 ^c , 1.95E+11 ^d

Continued

14.9583	$0_{5/2} - 668,525^o_{5/2}$	4.40E+10	6.87E+10 ^c , 6.60E+10 ^d
15.0089	$16,725_{3/2} - 682,998^o_{3/2}$	2.71E+11	2.71E+11 ^c , 2.42E+11 ^d
15.0125	$16,725_{3/2} - 682,838^o_{5/2}$	4.83E+10	5.94E+10 ^c , 5.60E+10 ^d
15.0544	$0_{5/2} - 664,256^o_{5/2}$	2.03E+11	2.44E+11 ^c , 2.38E+11 ^d
15.1021	$0_{5/2} - 662,160^o_{3/2}$	6.88E+09	1.29E+10 ^c , 1.30E+10 ^d
15.1291	$16,725_{3/2} - 677,704^o_{1/2}$	5.54E+09	8.27E+09 ^c , 8.00E+09 ^d
15.1747	$0_{5/2} - 658,993^o_{7/2}$	8.56E+10	8.94E+10 ^c , 8.60E+10 ^d
15.1762	$16,725_{3/2} - 675,652^o_{5/2}$	3.86E+10	4.46E+10 ^c , 4.00E+10 ^d
15.2058	$0_{5/2} - 657,645^o_{5/2}$	9.84E+10	1.12E+11 ^c , 1.10E+11 ^d
15.2830	$16,725_{3/2} - 671,045^o_{5/2}$	2.00E+10	1.37E+10 ^c , 1.30E+10 ^d
15.4433	$16,725_{3/2} - 664,256^o_{5/2}$	1.52E+10	1.31E+10 ^c , 1.20E+10 ^d
15.4588	$0_{5/2} - 646,880^o_{7/2}$	1.82E+09	3.07E+09 ^c , 3.00E+09 ^d
15.4680	$0_{5/2} - 646,494^o_{5/2}$	1.65E+10	2.05E+10 ^c , 1.90E+10 ^d
15.4934	$16,725_{3/2} - 662,160^o_{3/2}$	1.22E+10	1.41E+10 ^c , 1.30E+10 ^d

a: Ritz wavelengths calculated employing the experimental energy level values from [22]. Transitions are given by values (in cm⁻¹) of involved energy levels where subscripts denote their J-values. b: MCDHF values from [27]. pE + q = p.10^q. c: HFR values from [27]. d: Values taken from [24]. e: Values taken from [26].

3.1.2. Ion Xe¹⁰⁺

The main works on the spectrum analysis of Xe XI are contained in Refs [25] [26] [27] [28] where the authors used, on the one hand a low-inductance vacuum spark and a 10.7 m grazing-incidence spectrograph, and on the other hand the Hartree-Fock calculations and orthogonal parameters. They classified about 200 allowed lines belonging to $4d^8 - (4p^54d^9 + 4d^75p + 4d^74f)$ transition arrays in the 105 - 157 Å spectral range, established all the 9 levels of the $4d^8$ configuration and 123 levels of the $4p^54d^9 + 4d^75p + 4d^74f$ configurations. These researchers reported the HFR transition probabilities of the classified lines.

Employing the RCI method and the distorted wave approximation implemented in the Flexible Atomic Code (FAC) [46], Shen *et al.* [29] computed the energy levels, transition probabilities and electron impact collision strengths in Xe XI. The transition rates were given for allowed lines involving the first 400 fine-structure levels of their model. These authors, in comparing their calculated rates with respect to those by Churilov *et al.* [28] for 31 strong lines, estimated the accuracy of their data better than 20%.

We recently utilized two independent theoretical methods HFR and MCDHF/RCI to produce a set of radiative properties (transition probabilities and oscillator strengths) for 576 Xe XI allowed spectral lines pertaining to the $4d^8 - (4p^54d^9 + 4d^75p + 4d^74f)$ transition arrays in the EUV range 102-157 Å [29]. 87 out of those E1 transitions (about 15%) satisfy the reliability criteria (7).

Figure 1 displays the comparison between our HFR and MCDHF/RCI log

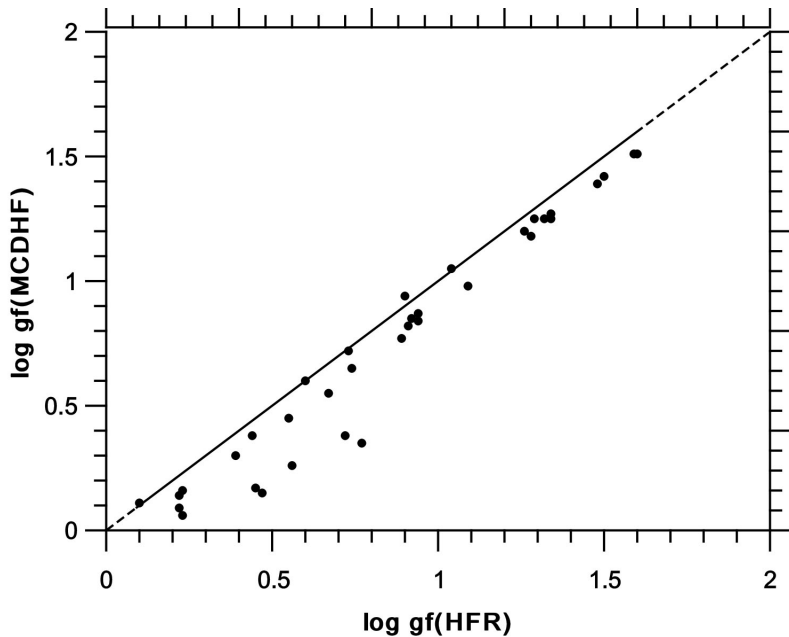


Figure 1. Comparison between our HFR and MCDHF oscillator strengths ($\log gf$) for Xe XI spectral lines [30]. Only transitions with $\log gf > 0$, $CF \geq 0.5$ and $0.9 \leq B/C \leq 1.10$ are shown in the figure.

gf-values (gf , weighted oscillator strength, $\sim gA$) for the strongest lines ($\log gf > 0$), and we can see that the MCDHF values are systematically smaller than the HFR ones. The average ratio $\langle gf(\text{MCDHF})/gf(\text{HFR}) \rangle$ being equal to 0.78 ± 0.19 , this systematic is thus about 20%. The observed trend is mainly explained by missing core-core and core-valence correlations related to missing configurations with more than one hole in the 4p core subshell in our HFR model.

In [Figure 2](#) and [Figure 3](#), the gA -values by Churilov *et al.* [28], who used a HFR approach but with smaller configuration sets, are compared respectively with our HFR and MCDHF/RCI data, in only considering the lines meeting the reliability criteria (7). [Figure 2](#) indicates that the extension of the CI expansions in our HFR model has a marginal effect on the transition rates, and we have actually found the average ratio $\langle gA([28])/gA(\text{HFR}) \rangle$ equal to 1.00 ± 0.02 . Therefore, as expected we also observe from [Figure 3](#) an about 20% systematic decrease on our MCDHF rates, for the strongest lines ($gA > 10^{12} \text{ s}^{-1}$), due to missing 4p subshell core-excited configurations in the Churilov *et al.*'s HFR model, with the average ratio $\langle gA(\text{MCDHF})/gA([28]) \rangle = 0.85 \pm 0.20$.

In comparing the FAC transition probabilities by Shen *et al.* [29] with respect to our HFR and MCDHF data [30] for the 31 strong lines presented in their table B, we have found respectively the average rate ratios $\langle gA([29])/gA(\text{HFR}) \rangle = 0.89 \pm 0.26$ and $\langle gA([29])/gA(\text{MCDHF}) \rangle = 1.41 \pm 0.94$. We conclude that the values of [29] appear to be overall about 10% smaller than our HFR results and 40% greater than our MCDHF data. The authors did not mention any information on the accuracy indicators (CF and B/C), the transition rates of the involved lines not satisfying the reliability criteria (7) could explain the high standard deviation

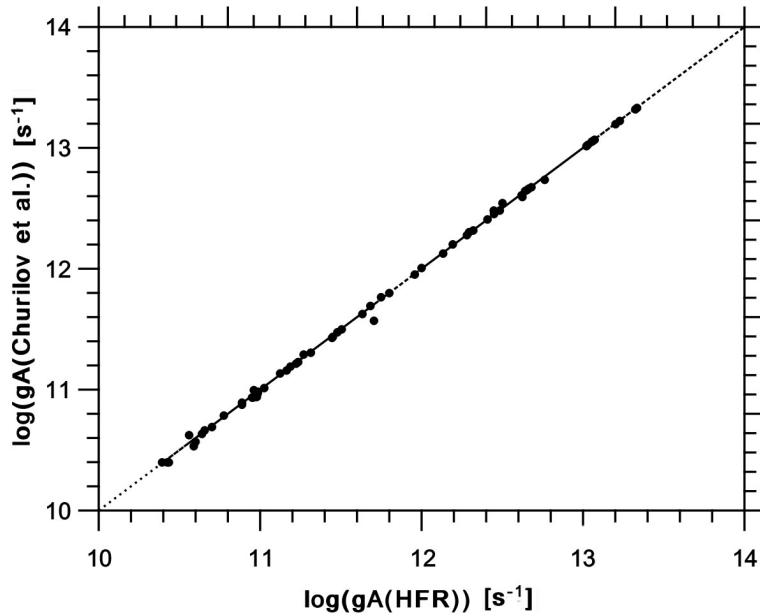


Figure 2. Comparison between the gA-values obtained from our HFR model [30] and the one by Churilov *et al.* [28] for Xe XI spectral lines. Only lines with weak cancellation effects ($CF > 0.05$) have been selected.

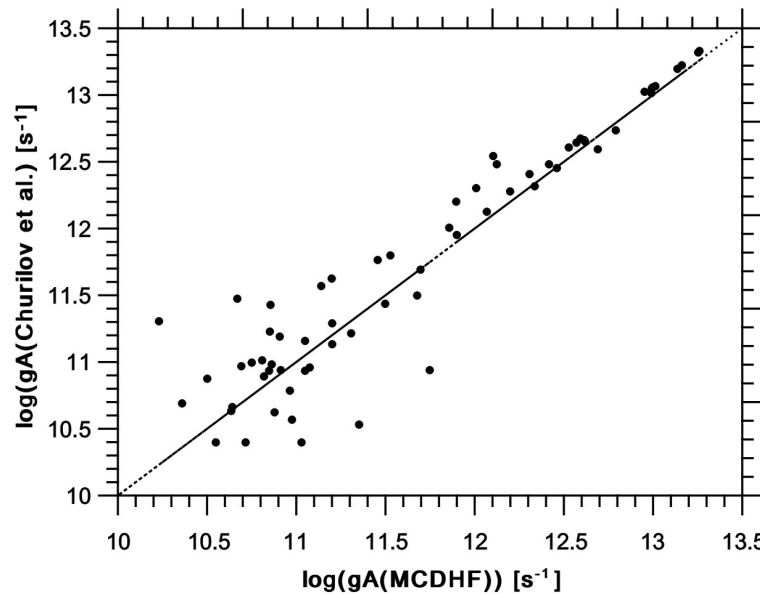


Figure 3. Comparison between the gA-values obtained in our MCDHF/RCI model [30] and the HFR model by Churilov *et al.* [28] for Xe XI spectral lines. Only lines with $CF > 0.05$ and $0.9 \leq B/C \leq 1.1$ have been selected.

of $\langle gA([29]) / gA(\text{MCDHF}) \rangle$. The large discrepancy observed with our MCDHF/RCI model results mainly from missing 4p subshell single, double and triple core-holes configurations in their physical model. The possible explanation of the small difference with our HFR model is the limitation of the correlations to the shell with the principal quantum number $n = 5$.

In the present work, the adopted transition probabilities are the MCDHF ones

from Bokamba *et al.* [30]. **Table 3** reports the adopted transition probabilities (column 3), and column 4 contains other available data [28] [29].

Table 3. Adopted transition probabilities (gA) in Xe XI, as well as other available gA-values.

λ (nm) ^a	Transition	Adopted gA (s^{-1}) ^b	Other gA (s^{-1})
10.3912	26,670 ₂ - 989,020 ₁ ⁰	1.20E+11	1.39E+11 ^c
10.5695	42,900 ₂ - 989,020 ₁ ⁰	8.33E+11	1.15E+12 ^c , 1.14E+12 ^d
10.6125	15,205 ₃ - 957,488 ₃ ⁰	7.20E+11	1.00E+12 ^c , 1.01E+12 ^d
10.6770	15,205 ₃ - 951,795 ₂ ⁰	8.35E+11	9.72E+11 ^c
10.7585	15,205 ₃ - 944,705 ₂ ⁰	5.09E+11	7.47E+11 ^c
10.8094	26,670 ₂ - 951,795 ₂ ⁰	7.36E+11	9.54E+11 ^c
10.8579	26,670 ₂ - 947,660 ₁ ⁰	2.38E+11	3.11E+11 ^c
10.8928	26,670 ₂ - 944,705 ₂ ⁰	1.39E+12	1.57E+12 ^c
10.9029	34,610 ₁ - 951,795 ₂ ⁰	2.61E+12	3.05E+12 ^c , 3.03E+12 ^d
10.9093	40,835 ₄ - 957,488 ₃ ⁰	8.96E+12	1.07E+13 ^c , 1.06E+13 ^d , 1.19E+13 ^e
10.9236	32,210 ₀ - 947,660 ₁ ⁰	4.71E+11	7.21E+11 ^c
10.9339	42,900 ₂ - 957,488 ₃ ⁰	1.17E+12	1.36E+12 ^c ; 1.34E+12 ^d
10.9577	0 ₄ - 912,600 ₃ ⁰	2.24E+11	2.24E+11 ^c
10.9655	13,140 ₂ - 925,010 ₁ ⁰	2.06E+11	2.86E+11 ^c
10.9879	34,610 ₁ - 944,705 ₂ ⁰	2.03E+12	2.56E+12 ^c , 2.56E+12 ^d
11.0024	42,900 ₂ - 951,795 ₂ ⁰	3.92E+12	4.79E+12 ^c , 4.72E+12 ^d
11.0085	0 ₄ - 908,390 ₃ ⁰	2.12E+11	4.49E+11 ^c
11.0528	26,670 ₂ - 931,420 ₁ ⁰	8.36E+11	1.53E+12 ^c
11.0889	42,900 ₂ - 944,705 ₂ ⁰	3.72E+12	4.38E+12 ^c , 4.40E+12 ^d
11.1001	88,130 ₀ - 989,020 ₁ ⁰	4.16E+12	4.50E+12 ^c , 4.48E+12 ^d
11.1178	13,140 ₂ - 912,600 ₃ ⁰	1.02E+12	1.97E+12 ^c , 2.01E+12 ^d
11.1209	32,210 ₀ - 931,420 ₁ ⁰	7.37E+11	2.05E+11 ^c
11.1268	34,610 ₁ - 933,343 ₀ ⁰	1.58E+12	1.91E+12 ^c , 1.90E+12 ^d
11.1294	13,140 ₂ - 911,665 ₂ ⁰	1.27E+12	3.17E+12 ^c , 3.49E+12 ^d
11.1316	26,670 ₂ - 925,010 ₁ ⁰	4.26E+11	4.75E+11 ^c
11.1380	26,670 ₂ - 924,500 ₂ ⁰	5.39E+12	6.60E+12 ^c
11.1384	40,835 ₄ - 938,628 ₅ ⁰	1.82E+13	2.16E+13 ^c , 2.14E+13 ^d , 2.43E+13 ^e
11.1434	15,205 ₃ - 912,600 ₃ ⁰	8.97E+12	9.86E+12 ^c
11.1435	0 ₄ - 897,383 ₅ ⁰	1.79E+13	2.11E+13 ^c , 2.08E+13 ^d , 2.36E+13 ^e
11.1506	34,610 ₁ - 931,420 ₁ ⁰	2.86E+12	3.64E+12 ^c
11.1550	15,205 ₃ - 911,665 ₂ ⁰	4.90E+12	4.21E+12 ^c ; 3.92E+12 ^d
11.1622	15,205 ₃ - 911,082 ₄ ⁰	1.45E+13	1.69E+13 ^c , 1.67E+13 ^d , 1.88E+13 ^e
11.1654	266,470 ₂ - 922,295 ₃ ⁰	1.03E+13	1.18E+13 ^c , 1.17E+13 ^d , 1.30E+13 ^e

Continued

11.1701	13,140 ₂ - 908,390 ₃ ^o	9.78E+12	1.05E+13 ^c , 1.03E+13 ^d , 7.76E+12 ^e
11.1739	0 ₄ - 894,941 ₃ ^o	9.84E+12	1.13E+13 ^c , 1.12E+13 ^d , 1.20E+13 ^e
11.1785	13,140 ₂ - 907,711 ₂ ^o	6.18E+12	5.79E+12 ^c , 5.44E+12 ^d
11.1832	40,835 ₄ - 935,035 ₃ ^o	7.94E+11	9.07E+11 ^c , 8.95E+11 ^d
11.1959	15,205 ₃ - 908,390 ₃ ^o	7.88E+11	1.56E+12 ^c , 1.59E+12 ^d
11.2007	32,210 ₀ - 925,010 ₁ ^o	3.37E+12	4.16E+12 ^c , 4.05E+12 ^d
11.2044	15,205 ₃ - 907,711 ₂ ^o	1.33E+12	2.80E+12 ^c , 3.03E+12 ^d
11.2055	0 ₄ - 892,420 ₄ ^o	1.37E+13	1.59E+13 ^c , 1.57E+13 ^d , 1.75E+13 ^e
11.2091	42,900 ₂ - 935,035 ₃ ^o	9.94E+12	1.15E+13 ^c , 1.14E+13 ^d , 1.19E+13 ^e
11.2373	34,610 ₁ - 924,500 ₂ ^o	2.17E+12	2.09E+12 ^c , 2.07E+12 ^d
11.2431	13,140 ₂ - 902,577 ₁ ^o	4.11E+12	4.61E+12 ^c , 4.60E+12 ^d
11.2713	26,670 ₂ - 913,877 ₁ ^o	2.89E+12	2.81E+12 ^c , 2.84E+12 ^d
11.3448	40,835 ₄ - 922,295 ₃ ^o	4.34E+11	7.72E+11 ^c
11.5266	40,835 ₄ - 908,390 ₃ ^o	2.57E+11	3.05E+11 ^c
12.7610	40,835 ₄ - 824,474 ₃ ^o	1.59E+11	1.33E+11 ^c , 1.36E+11 ^d
13.0443	15,205 ₃ - 781,822 ₂ ^o	6.59E+10	7.72E+10 ^c , 7.80E+10 ^d
13.1360	0 ₄ - 761,266 ₃ ^o	7.03E+10	2.43E+10 ^c
13.1978	34,610 ₁ - 792,311 ₀ ^o	2.29E+10	2.43E+10 ^c , 4.90E+10 ^d
13.2573	40,835 ₄ - 795,135 ₃ ^o	4.97E+11	4.82E+11 ^c , 4.92E+11 ^d , 3.07E+11 ^e
13.2664	34,610 ₁ - 788,396 ₁ ^o	8.49E+10	6.68E+10 ^c
13.2708	34,610 ₁ - 788,145 ₂ ^o	4.85E+10	2.20E+10 ^c
13.2785	42,900 ₂ - 795,995 ₂ ^o	9.21E+10	5.96E+10 ^c , 6.10E+10 ^d
13.2984	34,610 ₁ - 786,580 ₂ ^o	7.11E+10	1.72E+11 ^c , 1.69E+11 ^d , 1.09E+11 ^e
13.3361	15,205 ₃ - 765,052 ₂ ^o	8.19E+10	9.37E+10 ^c , 8.70E+10 ^d
13.3518	13,140 ₂ - 762,105 ₂ ^o	1.12E+11	8.91E+10 ^c , 8.60E+10 ^d
13.3655	40,835 ₄ - 789,029 ₅ ^o	3.15E+11	2.82E+11 ^c , 2.73E+11 ^d , 2.59E+11 ^e
13.3887	15,205 ₃ - 762,105 ₂ ^o	4.38E+10	4.53E+10 ^c , 4.60E+10 ^d
13.3968	0 ₄ - 746,445 ₃ ^o	7.56E+10	3.63E+10 ^c , 4.20E+10 ^d
13.4037	15,205 ₃ - 761,266 ₃ ^o	4.67E+10	3.01E+11 ^c , 2.98E+11 ^d , 2.26E+11 ^e
13.4184	42,900 ₂ - 788,145 ₂ ^o	6.44E+10	1.06E+11 ^c
13.4584	13,140 ₂ - 756,170 ₂ ^o	1.59E+11	1.86E+11 ^c , 1.95E+11 ^d , 1.35E+11 ^e
13.4622	32,210 ₀ - 775,030 ₁ ^o	3.54E+10	2.47E+10 ^c , 2.50E+10 ^d
13.4747	88,130 ₀ - 830,260 ₁ ^o	1.76E+11	2.06E+11 ^c , 2.02E+11 ^d , 1.71E+11 ^e
13.4843	13,140 ₂ - 754,745 ₁ ^o	1.12E+11	1.46E+11 ^c , 1.44E+11 ^d , 1.13E+11 ^e
13.4928	42,900 ₂ - 784,035 ₁ ^o	2.03E+11	1.67E+11 ^c , 1.64E+11 ^d , 1.90E+11 ^e
13.4987	15,205 ₃ - 756,016 ₄ ^o	2.86E+11	5.61E+11 ^c , 5.81E+11 ^d , 3.80E+11 ^e
13.5072	0 ₄ - 740,348 ₅ ^o	3.37E+11	6.31E+11 ^c , 6.29E+11 ^d , 5.96E+11 ^e

Continued

13.5198	15,205 ₃ - 754,860 ₃ ^o	2.25E+11	3.88E+10 ^c , 3.40E+10 ^d
13.5315	13,140 ₂ - 752,155 ₁ ^o	7.28E+10	9.7E+10 ^c , 9.60E+10 ^d
13.5614	0 ₄ - 737,388 ₄ ^o	4.76E+11	3.20E+11 ^c , 3.15E+11 ^d , 4.17E+11 ^e
13.5998	15,205 ₃ - 750,512 ₂ ^o	1.19E+11	9.54E+10 ^c
13.6025	32,210 ₀ - 767,369 ₁ ^o	3.17E+10	7.72E+10 ^c , 7.50E+10 ^d
13.6213	15,205 ₃ - 749,351 ₃ ^o	7.17E+10	2.79E+11 ^c , 2.68E+11 ^d , 2.24E+11 ^e
13.6401	40,835 ₄ - 773,968 ₅ ^o	5.60E+11	9.54E+10 ^c , 8.70E+10 ^d
13.6401	40,835 ₄ - 773,968 ₄ ^o	1.38E+11	5.07E+11 ^c , 3.71E+11 ^d
13.6588	42,900 ₂ - 775,030 ₁ ^o	7.04E+10	9.03E+10 ^c , 8.60E+10 ^d
13.6674	26,670 ₂ - 758,337 ₁ ^o	5.63E+10	9.41E+10 ^c , 9.90E+10 ^d
13.6713	0 ₄ - 731,458 ₄ ^o	1.58E+11	4.30E+11 ^c , 4.22E+11 ^d
13.6734	15,205 ₃ - 746,552 ₂ ^o	1.07E+11	2.72E+10 ^c , 2.50E+10 ^d
13.7238	13,140 ₂ - 741,800 ₃ ^o	8.08E+10	1.54E+11 ^c , 1.55E+11 ^d , 6.09E+10 ^e
13.8174	34,610 ₁ - 758,337 ₁ ^o	4.92E+10	9.65E+10 ^c , 9.30E+10 ^d
13.8889	88,130 ₀ - 808,130 ₁ ^o	5.2E+10	2.66E+10 ^c , 2.50E+10 ^d
13.8899	32,210 ₀ - 752,155 ₁ ^o	4.32E+10	4.36E+10 ^c , 4.30E+10 ^d
13.9684	34,610 ₁ - 750,512 ₂ ^o	9.46E+10	3.98E+10 ^c , 3.70E+10 ^d
14.3698	88,130 ₀ - 784,035 ₁ ^o	8.24E+09	8.47E+09 ^c
14.4881	88,130 ₀ - 778,350 ₁ ^o	2.85E+09	2.27E+09 ^c

a: Ritz wavelengths calculated employing the experimental energy level values from [28].
 Transitions are given by values (in cm⁻¹) of involved energy levels where subscripts denote their J-values. b: MCDHF values from [30]. pE + q = p·10^q. c: HFR values from [30].
 d: Values taken from [28]. e: Values taken from [29].

3.2. Ions of Er I Isoelectronic Sequence: Lu³⁺, Hf⁴⁺ and Ta⁵⁺

Investigations on the spectra of these three ions were performed at the National Bureau of Standards (NBS) [47] [48] [49] [50] [51] by means of, on the one hand, sliding-spark discharges and the grating spectrograph, and on the other hand semi-empirical parametric models of the corresponding atomic energy level structures. These authors did not publish any transition rates!

Radiative rates in these ions are very scarce, the only few data available in the literature, to our knowledge, are those by Anisimova *et al.* [36], Loginov and Tuchkin [37] and Bokamba *et al.* [38]. The first data are E1 transition probabilities on the transition arrays 4f¹³ns-4f¹³6p (n = 6.7) in Lu IV and Hf V computed by Anisimova *et al.* [36], ANI, using the Newton and least-squares monoconfigurational methods and those determined by Loginov and Tuchkin [37], LOG, employing the same methods for the transition arrays 4f¹⁴-4f¹³5d and 4f¹³6p-4f¹³5d in Lu IV, Hf V and Ta IV that neglect the configuration interaction. More recently, we obtained sets of radiative properties (transition probabilities and oscillator strengths) in Lu IV, Hf V and Ta IV for allowed transitions using the two independent theoretical atomic structure computational approaches HFR and

MCDHF/RCI [38].

3.2.1. Ion Lu³⁺

As for Lu IV, Sugar and Kaufman [47] classified 180 lines falling in the region 877 - 2128 Å, determined 57 energy levels of 4f¹⁴, 4f¹³5d, 4f¹³6s, 4f¹³6p, 4f¹³6d and 4f¹³7s configurations. Nine years later, Wyart *et al.* [51], in analyzing the 4f¹³5f configuration in the isoelectronic sequence of Yb III, classified 97 lines and established 13 energy levels of this configuration.

Recently, we used the theoretical approaches HFR and MCDHF/RCI to obtain a set of transition probabilities and oscillator strengths for 593 allowed spectral lines in the range 400 Å - 45 μm [38]. 179 out of those E1 transitions (about 30%) meet reliability criteria (7).

Figure 4 displays the comparison between our HFR and MCDHF/RCI oscillator strengths, for the strongest lines ($\log gf > 0$), with an average ratio $\langle \log(gf(\text{MCDHF})/\log(gf(\text{HFR})) \rangle = 0.95 \pm 0.22$ [38], *i.e.* MCDHF log (gf)-values are overall about 5% smaller than those obtained by HFR, and this systematics may be attributed to missing configurations with two holes in the 5p subshell in our the HFR-model expansions.

When comparing our MCDHF/RCI gA-values [38], for the strongest lines ($gA > 10^9 \text{ s}^{-1}$), with respect to those published by Anisimova *et al.* [36] and Loginov and Tuchkin [37] utilizing monoconfigurational approaches (Newton and least-squares methods stand for 1 and 2, respectively), we have found these average ratios $\langle gA(\text{ANI1})/gA(\text{MCDHF}) \rangle = 1.21 \pm 0.48$, $\langle gA(\text{ANI2})/gA(\text{MCDHF}) \rangle = 1.20 \pm 0.45$, $\langle gA(\text{LOG1})/gA(\text{MCDHF}) \rangle = 0.96 \pm 0.24$, $\langle gA(\text{LOG2})/gA(\text{MCDHF}) \rangle = 0.97 \pm 0.24$ [38], which shows the necessity to take into account the configuration interaction in calculations. **Figure 5** illustrates these comparisons.

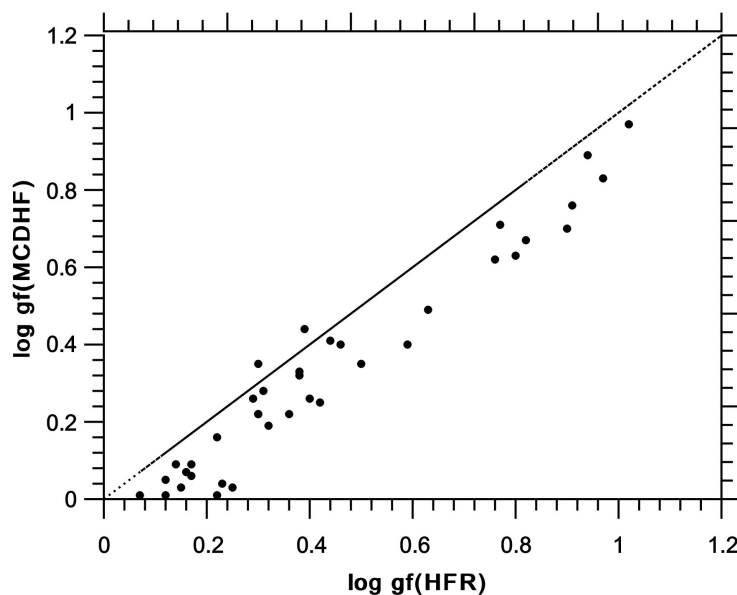


Figure 4. Comparison between our HFR and MCDHF/RCI oscillator strengths ($\log gf$) for Lu IV spectral lines [38]. Only transitions with $\log gf > 0$, $CF \geq 0.5$ and $0.9 \leq B/C \leq 1.10$ have been selected.

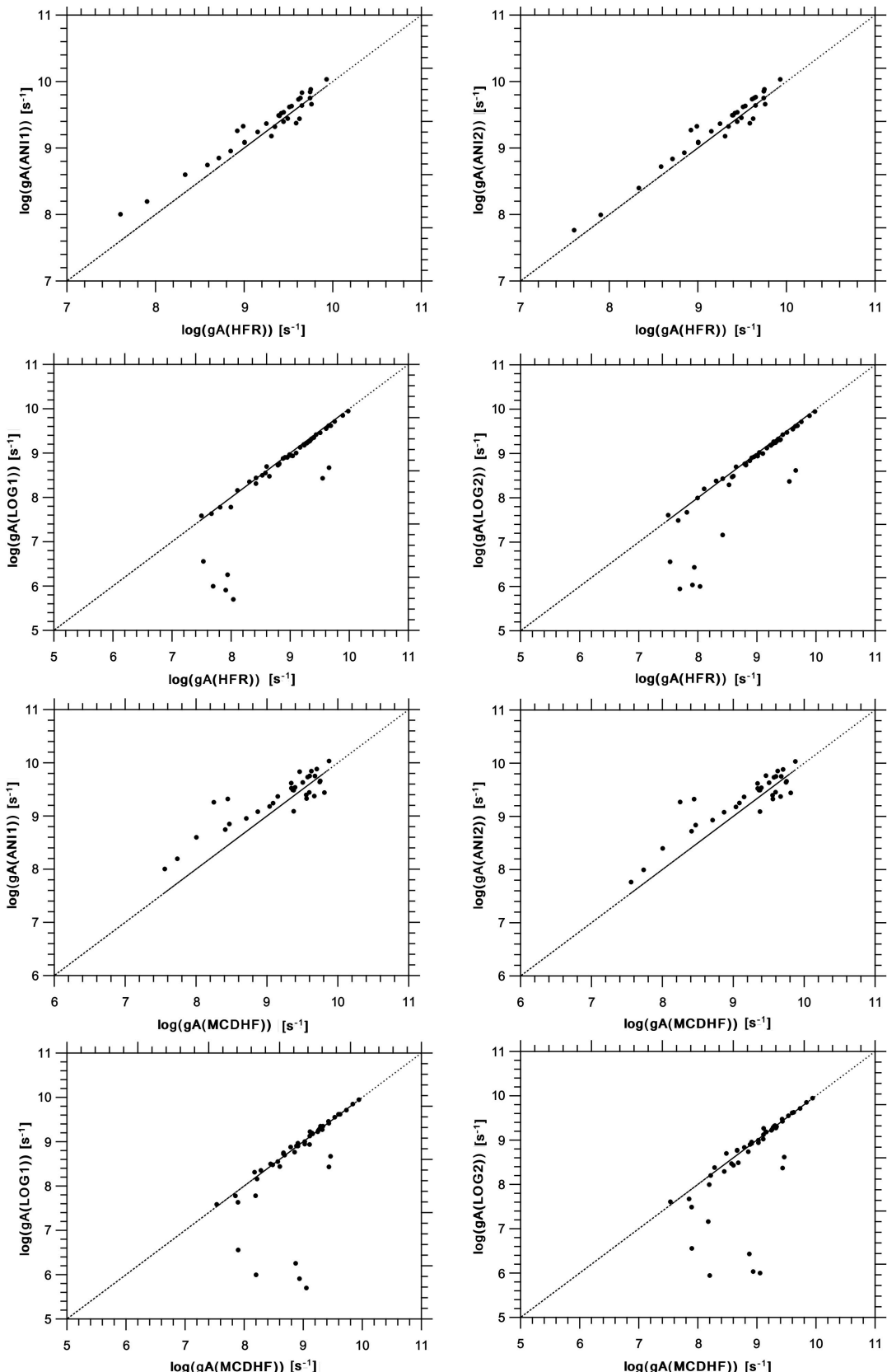


Figure 5. Comparison between our MCDHF/RCI gA-values [38] with the available data [36] [37] for Lu IV spectral lines. Only transitions with $\log gf > 0$, $CF \geq 0.5$ and $0.9 \leq B/C \leq 1.10$ have been retained.

In making the similar comparisons employing here our HFR model, we have $\langle gA(ANI1)/gA(HFR) \rangle = 1.09 \pm 0.26$, $\langle gA(ANI2)/gA(HFR) \rangle = 1.09 \pm 0.25$, $\langle gA(LOG1)/gA(HFR) \rangle = 0.91 \pm 0.14$, $\langle gA(LOG2)/gA(HFR) \rangle = 0.89 \pm 0.22$ [38], which is also illustrated in [Figure 5](#). In this case, we emphasize the importance of CI in calculations, as well.

In the present work, the recommended transition probabilities in Lu^{3+} are the MCDHF data from Bokamba *et al.* [38], and they are reported in [Table 4](#) (column 3) along with other available data (column 4) [36] [37].

Table 4. Adopted transition probabilities (gA) in Lu IV, as well as other available gA-values.

λ (nm) ^a	Transition	Adopted gA (s^{-1}) ^b	Other gA (s^{-1})
60.8995	98,505.0 ₁ ⁰ - 262,710.1 ₂	3.26E+08	6.65E+08 ^c
61.0993	98,505.0 ₁ ⁰ - 262,173.0 ₂	2.99E+09	1.88E+09 ^c
62.5764	102,216.6 ₄ ⁰ - 262,021.3 ₅	8.20E+09	4.25E+09 ^c
62.5959	90,432.9 ₂ ⁰ - 250,187.8 ₂	3.15E+08	1.36E+10 ^c
64.2169	94,768.1 ₅ ⁰ - 250,490.3 ₆	6.99E+10	7.79E+10 ^c
64.2506	106,380.6 ₄ ⁰ - 262,021.3 ₅	5.00E+10	5.08E+10 ^c
64.5875	107,986.6 ₂ ⁰ - 262,815.4 ₃	1.03E+10	9.81E+09 ^c
65.5141	98,239.3 ₆ ⁰ - 250,878.2 ₅	5.16E+08	7.67E+08 ^c
65.6514	98,558.5 ₄ ⁰ - 250,878.2 ₅	2.95E+10	3.88E+10 ^c
65.6810	98,239.3 ₆ ⁰ - 250,490.3 ₆	1.13E+09	2.07E+09 ^c
65.6854	98,558.5 ₄ ⁰ - 250,799.3 ₄	1.47E+10	2.27E+10 ^c
65.8536	110,858.0 ₁ ⁰ - 262,710.1 ₂	6.21E+09	3.73E+09 ^c
65.9221	111,377.8 ₅ ⁰ - 263,072.0 ₅	1.08E+10	1.02E+10 ^c
66.0635	99,660.0 ₂ ⁰ - 251,029.6 ₃	1.43E+10	1.62E+10 ^c
66.0873	110,858.0 ₁ ⁰ - 262,173.0 ₂	8.41E+09	1.17E+10 ^c
66.2441	111,377.8 ₅ ⁰ - 262,334.7 ₆	7.08E+10	7.24E+10 ^c
66.2700	111,812.3 ₃ ⁰ - 262,710.1 ₂	2.94E+09	3.60E+09 ^c
66.3819	111,377.8 ₅ ⁰ - 262,021.3 ₅	1.12E+09	1.05E+09 ^c
66.5855	112,632.5 ₂ ⁰ - 262,815.4 ₃	1.33E+10	1.23E+10 ^c
66.8715	112,632.5 ₂ ⁰ - 262,173.0 ₂	1.04E+10	1.25E+10 ^c
67.1524	102,216.6 ₄ ⁰ - 251,131.7 ₅	2.86E+10	3.65E+10 ^c
67.2669	102,216.6 ₄ ⁰ - 250,878.2 ₅	1.01E+10	6.96E+09 ^c
67.2673	114,049.4 ₁ ⁰ - 262,710.1 ₂	2.88E+09	3.34E+09 ^c
67.4596	103,070.4 ₃ ⁰ - 251,307.3 ₄	2.25E+10	2.84E+10 ^c
67.5112	114,049.4 ₁ ⁰ - 262,173.0 ₂	1.37E+09	9.12E+08 ^c
67.5323	114,632.8 ₃ ⁰ - 262,710.1 ₂	8.05E+07	4.99E+08 ^c
67.7491	115,468.5 ₄ ⁰ - 263,072.0 ₅	4.82E+10	5.22E+10 ^c

Continued

67.7781	114,632.8 ₃ ^o	- 262,173.0 ₂	1.30E+09	1.85E+09 ^c
67.9729	103,070.4 ₃ ^o	- 250,187.8 ₂	2.87E+09	1.35E+09 ^c
68.1702	103,798.7 ₅ ^o	- 250,490.3 ₆	2.41E+09	9.44E+08 ^c
68.2348	115,468.5 ₄ ^o	- 262,021.3 ₅	1.02E+09	8.95E+08 ^c
68.3649	116,798.2 ₄ ^o	- 263,072.0 ₅	9.78E+08	2.36E+08 ^c
68.8596	116,798.2 ₄ ^o	- 262,021.3 ₅	3.04E+07	6.27E+07 ^c
69.0004	106,380.6 ₄ ^o	- 251,307.3 ₄	2.76E+09	1.76E+09 ^c
69.0317	117,312.0 ₃ ^o	- 262,173.0 ₂	5.39E+08	2.71E+07 ^c
69.0317	117,312.0 ₃ ^o	- 262,173.0 ₂	5.39E+08	2.71E+07 ^c
69.0841	106,380.6 ₄ ^o	- 251,131.7 ₅	2.97E+09	2.18E+09 ^c
69.1329	106,380.6 ₄ ^o	- 251,029.6 ₃	3.39E+08	2.14E+08 ^c
69.2053	106,380.6 ₄ ^o	- 250,878.2 ₅	4.75E+09	1.96E+09 ^c
74.4923	128,573.3 ₂ ^o	- 262,815.4 ₃	4.89E+07	8.37E+07 ^c
74.6295	117,312.0 ₃ ^o	- 251,307.3 ₄	1.68E+08	6.45E+07 ^c
81.7138	128,929.0 ₃ ^o	- 251,307.3 ₄	1.77E+07	1.98E+07 ^c
114.3092	98,505.0 ₁ ^o	- 185,987.0 ₂	1.92E+08	2.04E+08 ^c , 2.25E+08 ^d , 2.40E+08 ^c
116.6854	98,505.0 ₁ ^o	- 184,205.5 ₁	1.65E+08	1.28E+08 ^c , 1.44E+08 ^d , 1.59E+08 ^c
124.7521	106,380.6 ₄ ^o	- 186,539.6 ₃	4.62E+08	6.20E+08 ^c , 5.32E+08 ^d , 5.81E+08 ^c
124.8100	94,768.1 ₅ ^o	- 174,889.9 ₄	6.12E+08	7.57E+08 ^c , 7.56E+08 ^d , 6.84E+08 ^c
126.4913	105,148.7 ₀ ^o	- 184,205.5 ₁	7.67E+08	8.17E+08 ^c , 8.01E+08 ^d , 7.98E+08 ^c
126.6156	106,380.6 ₄ ^o	- 185,359.8 ₄	2.90E+08	4.54E+08 ^c
127.3026	107,986.6 ₂ ^o	- 186,539.6 ₃	7.14E+08	6.52E+08 ^c , 5.81E+08 ^d , 5.46E+08 ^c
127.4770	94,768.1 ₅ ^o	- 173,213.6 ₅	4.63E+08	6.48E+08 ^c , 5.61E+08 ^d , 5.94E+08 ^c
127.6543	98,505.0 ₁ ^o	- 176,841.6 ₂	4.01E+08	2.64E+08 ^c , 2.75E+08 ^d , 2.70E+08 ^c
128.9386	97,333.6 ₃ ^o	- 174,889.9 ₄	1.06E+09	1.03E+09 ^c , 8.82E+08 ^d , 8.73E+08 ^c
130.3856	99,660.0 ₂ ^o	- 176,355.6 ₃	3.43E+07	3.15E+07 ^c , 3.85E+07 ^d , 4.06E+07 ^c
131.0077	98,558.5 ₄ ^o	- 174,889.9 ₄	1.28E+09	1.10E+09 ^c , 8.64E+08 ^d , 1.05E+09 ^c
132.3019	98,558.5 ₄ ^o	- 174,143.2 ₃	2.80E+08	3.37E+08 ^c , 3.15E+08 ^d , 1.96E+08 ^c
133.1044	110,858.0 ₁ ^o	- 185,987.0 ₂	3.71E+08	3.81E+08 ^c , 3.55E+08 ^d , 2.95E+08 ^c
133.3790	98,239.3 ₆ ^o	- 173,213.6 ₅	8.74E+09	9.59E+09 ^c , 8.84E+09 ^d , 8.83E+09 ^c
133.4946	98,505.0 ₁ ^o	- 173,414.4 ₂	1.41E+09	1.70E+09 ^c , 1.57E+09 ^d , 1.55E+09 ^c
133.8199	111,812.3 ₃ ^o	- 186,539.6 ₃	4.84E+08	3.99E+08 ^c , 4.97E+08 ^d , 3.08E+08 ^c
135.1680	111,377.8 ₅ ^o	- 185,359.8 ₄	6.89E+09	7.76E+09 ^c , 7.06E+09 ^d , 7.09E+09 ^c
135.3741	90,432.9 ₂ ^o	- 164,302.3 ₃	2.71E+09	2.74E+09 ^c , 2.60E+09 ^d , 2.65E+09 ^c
135.5517	164,728.5 ₄ ^o	- 238,501.1 ₄ ^o	1.60E+09	1.44E+09 ^c
135.5851	99,660.0 ₂ ^o	- 173,414.4 ₂	2.02E+09	2.29E+09 ^c , 2.10E+09 ^d , 2.13E+09 ^c

Continued

135.7875	164,302.3 ₃ ^o - 237,946.8 ₂	7.68E+08	9.27E+08 ^c
135.8725	176,355.6 ₃ ^o - 249,954.0 ₂ ^o	4.52E+08	1.42E+08 ^c
135.9666	111,812.3 ₃ ^o - 185,359.8 ₄	2.72E+08	3.54E+08 ^c
136.3243	112,632.5 ₂ ^o - 185,987.0 ₂	2.10E+09	2.15E+09 ^c , 1.87E+09 ^d , 1.88E+09 ^e
136.3373	110,858.0 ₁ ^o - 184,205.5 ₁	1.29E+09	1.47E+09 ^c , 1.34E+09 ^d , 1.32E+09 ^e
136.3756	176,355.6 ₃ ^o - 249,682.5 ₃ ^o	5.71E+09	5.58E+09 ^c
137.1498	164,302.3 ₃ ^o - 237,215.3 ₃	1.03E+10	1.15E+10 ^c
137.2855	176,841.6 ₂ ^o - 249,682.5 ₃ ^o	5.45E+09	3.58E+09 ^c
137.5357	164,728.5 ₄ ^o - 237,436.9 ₄ ^o	5.03E+09	9.08E+09 ^c
137.6021	102,216.6 ₄ ^o - 174,889.9 ₄	2.15E+09	2.46E+09 ^c , 2.23E+09 ^d , 2.02E+09 ^e
137.6114	176,841.6 ₂ ^o - 249,510.0 ₁ ^o	5.37E+09	5.86E+09 ^c
137.7215	176,355.6 ₃ ^o - 248,965.9 ₃ ^o	1.78E+09	8.36E+08 ^c , 1.81E+09 ^d , 1.86E+09 ^e
138.1632	164,728.5 ₄ ^o - 237,215.3 ₃ ^o	1.30E+09	3.97E+09 ^c
137.9562	164,728.5 ₄ ^o - 237,106.7 ₃	5.55E+09	4.48E+09 ^c , 4.35E+09 ^d , 4.37E+09 ^e
138.3185	164,728.5 ₄ ^o - 237,025.4 ₄ ^o	4.65E+09	3.86E+09 ^c , 2.37E+09 ^d , 2.36E+09 ^e
138.3798	176,355.6 ₃ ^o - 248,620.5 ₂ ^o	4.18E+09	1.27E+09 ^c
138.9850	176,355.6 ₃ ^o - 248,305.8 ₄ ^o	1.69E+10	2.05E+10 ^c
139.0074	164,728.5 ₄ ^o - 236,667.1 ₅ ^o	2.11E+10	2.59E+10 ^c
139.0094	114,049.4 ₁ ^o - 185,987.0 ₂	1.50E+08	2.63E+08 ^c , 2.05E+08 ^d , 1.45E+07 ^e
139.0306	102,216.6 ₄ ^o - 174,143.2 ₃	2.67E+09	3.22E+09 ^c , 2.87E+09 ^d , 2.98E+09 ^e
139.0689	114,632.8 ₃ ^o - 186,539.6 ₃	1.30E+09	1.92E+09 ^c , 1.68E+09 ^d , 1.84E+09 ^e
139.7175	112,632.5 ₂ ^o - 184,205.5 ₁	8.12E+08	9.75E+08 ^c , 9.24E+08 ^d , 9.03E+08 ^e
140.1318	164,302.3 ₃ ^o - 235,663.7 ₂	9.37E+09	1.13E+10 ^c
140.1459	114,632.8 ₃ ^o - 185,987.0 ₂	1.96E+09	2.51E+09 ^c , 2.24E+09 ^d , 2.07E+09 ^e
140.6644	103,798.7 ₅ ^o - 174,889.9 ₄	4.20E+09	4.86E+09 ^c , 4.15E+09 ^d , 4.23E+09 ^e
140.7042	115,468.5 ₄ ^o - 186,539.6 ₃	3.41E+09	4.06E+09 ^c , 3.56E+09 ^d , 3.54E+09 ^e
142.1585	103,070.4 ₃ ^o - 173,414.4 ₂	1.06E+09	1.26E+09 ^c , 1.01E+09 ^d , 9.95E+08 ^e
142.9082	106,380.6 ₄ ^o - 176,355.6 ₃	3.95E+09	4.49E+09 ^c , 4.15E+09 ^d , 4.12E+09 ^e
142.9380	94,768.1 ₅ ^o - 164,728.5 ₄	5.38E+09	5.65E+09 ^c , 5.16E+09 ^d , 5.18E+09 ^e
143.0793	115,468.5 ₄ ^o - 185,359.8 ₄	1.44E+09	1.73E+09 ^c , 1.50E+09 ^d , 1.52E+09 ^e
144.0613	103,798.7 ₅ ^o - 173,213.6 ₅	1.88E+09	2.18E+09 ^c , 1.93E+09 ^d , 1.93E+09 ^e
145.2327	107,986.6 ₂ ^o - 176,841.6 ₂	1.76E+09	1.86E+09 ^c , 1.68E+09 ^d , 1.67E+09 ^e
145.9656	106,380.6 ₄ ^o - 174,889.9 ₄	1.56E+08	9.90E+07 ^c , 6.03E+07 ^d , 9.90E+07 ^e
151.1259	98,558.5 ₄ ^o - 164,728.5 ₄	1.81E+09	2.06E+09 ^c , 1.81E+09 ^d , 1.75E+09 ^e
152.0947	184,205.5 ₁ ^o - 249,954.0 ₂ ^o	3.98E+09	3.26E+09 ^c
152.0947	184,205.5 ₁ ^o - 249,954.0 ₂ ^o	3.98E+09	3.26E+09 ^c

Continued

152.2207	173,213.6 ₅ - 238,907.7 ₅ ^o	7.09E+09	7.04E+09 ^c
152.8358	185,359.8 ₄ - 250,789.5 ₄ ^o	5.14E+09	4.26E+09 ^c
153.0782	173,414.4 ₄ - 238,740.5 ₃ ^o	3.56E+09	3.30E+09 ^c
153.1288	184,205.5 ₁ - 249,510.0 ₁ ^o	2.87E+08	1.74E+09 ^c
153.1687	173,213.6 ₅ - 238,501.1 ₄ ^o	5.39E+08	4.19E+08 ^c
154.9609	173,414.4 ₂ - 237,946.8 ₂ ^o	6.08E+09	6.30E+09 ^c
155.1588	173,213.6 ₅ - 237,663.7 ₆ ^o	2.44E+10	2.56E+10 ^c
155.2433	184,205.5 ₁ - 248,620.5 ₂ ^o	1.48E+09	2.12E+08 ^c
155.3779	185,359.8 ₄ - 249,719.0 ₅ ^o	2.05E+10	2.16E+10 ^c
155.4661	185,359.8 ₄ - 249,682.5 ₃ ^o	1.15E+09	1.30E+08 ^c
155.6423	186,539.6 ₃ - 250,789.5 ₄ ^o	1.10E+10	9.29E+09 ^c
155.7067	173,213.6 ₅ - 237,436.9 ₄ ^o	3.88E+09	2.04E+09 ^c
156.3306	185,987.0 ₂ - 249,954.0 ₄ ^o	3.95E+09	4.95E+09 ^c
156.6156	174,889.9 ₄ - 238,740.5 ₃ ^o	1.14E+09	1.44E+09 ^c
156.7108	173,213.6 ₅ - 237,025.4 ₄ ^o	4.75E+09	5.54E+09 ^c , 5.64E+09 ^d , 5.64E+09 ^e
156.7310	174,143.2 ₃ - 237,946.8 ₂ ^o	2.38E+09	2.60E+09 ^c
157.0049	173,414.4 ₂ - 237,106.7 ₃ ^o	3.58E+09	2.78E+09 ^c , 2.49E+09 ^d , 2.49E+09 ^e
157.2050	174,889.9 ₄ - 238,501.1 ₄ ^o	5.09E+09	6.01E+09 ^c
157.2176	185,359.8 ₄ - 248,965.9 ₃ ^o	5.64E+09	5.75E+09 ^c , 4.56E+09 ^d , 4.56E+09 ^e
157.5957	173,213.6 ₅ - 236,667.1 ₅ ^o	1.28E+09	1.50E+09 ^c
157.6929	186,539.6 ₃ - 249,954.0 ₂ ^o	9.80E+08	1.02E+09 ^c
158.5349	111,812.3 ₃ ^o - 174,889.9 ₂	7.91E+07	3.39E+07 ^c , 3.60E+06 ^d , 3.60E+06 ^e
158.8222	174,143.2 ₃ - 174,889.9 ₂ ^o	3.95E+09	3.10E+09 ^c , 2.77E+09 ^d , 2.85E+09 ^e
158.8663	185,359.8 ₄ - 248,305.8 ₄ ^o	1.03E+09	1.20E+09 ^c
158.9481	185,987.0 ₂ - 248,900.6 ₂ ^o	2.80E+08	2.22E+09 ^c , 2.09E+09 ^d , 2.11E+09 ^e
159.8558	110,858.0 ₁ ^o - 173,414.4 ₂	7.11E+07	6.52E+07 ^c , 6.00E+07 ^d , 4.70E+07 ^e
160.1889	186,539.6 ₃ - 248,965.9 ₃ ^o	3.62E+09	9.75E+08 ^c , 2.13E+09 ^d , 2.12E+09 ^e
160.3566	186,539.6 ₃ - 248,900.6 ₂ ^o	2.38E+09	1.01E+09 ^c , 1.23E+09 ^d , 1.23E+09 ^e
160.4482	174,889.9 ₄ - 237,215.3 ₃ ^o	3.14E+09	1.90E+09 ^c
160.7283	174,889.9 ₄ - 237,106.7 ₃ ^o	1.09E+09	2.03E+09 ^c , 1.51E+09 ^d , 1,51E+09 ^e
160.9386	174,889.9 ₄ - 237,025.4 ₄ ^o	6.46E+09	4.21E+09 ^c , 2.75E+09 ^d , 2,76E+09 ^e
161.0801	186,539.6 ₃ - 248,620.5 ₂ ^o	3.32E+08	1.58E+09 ^c
161.7186	111,377.8 ₅ ^o - 173,213.6 ₅	7.85E+07	4.65E+07 ^c , 4.29E+07 ^d , 3.08E+07 ^e
161.9009	186,539.6 ₃ - 248,305.8 ₄ ^o	1.11E+09	1.08E+09 ^c
162.3609	176,355.6 ₃ - 237,946.8 ₂ ^o	6.61E+07	9.30E+07 ^c
162.5474	174,143.2 ₃ - 235,663.7 ₂ ^o	1.15E+09	1.27E+09 ^c

Continued

165.9556	114,632.8 ₃ ⁰	- 174,889.9 ₄	7.44E+08	8.71E+07 ^c , 1.80E+06 ^d , 2.70E+06 ^e
167.9053	116,798.2 ₄ ⁰	- 176,355.6 ₃	3.62E+07	4.02E+07 ^c , 1.01E+08 ^d , 5.81E+07 ^e
169.3664	117,312.0 ₃ ⁰	- 176,355.6 ₃	1.01E+08	2.16E+08 ^c , 3.97E+08 ^d , 2.50E+08 ^e
170.1213	114,632.8 ₃ ⁰	- 173,414.4 ₂	1.13E+09	1.09E+08 ^c , 5.00E+05 ^d , 1.00E+06 ^e
172.1416	116,798.2 ₄ ⁰	- 174,889.9 ₄	5.04E+09	5.64E+09 ^c , 7.62E+09 ^d , 7.63E+09 ^e
172.5140	128,573.3 ₂ ⁰	- 186,539.6 ₃	2.21E+09	2.62E+09 ^c , 3.33E+09 ^d , 3.35E+09 ^e
173.1749	115,468.5 ₄ ⁰	- 173,213.6 ₅	1.59E+08	4.96E+07 ^c , 9.90E+05 ^d , 8.80E+05 ^e
173.5792	128,929.0 ₃ ⁰	- 186,539.6 ₃	4.00E+09	4.31E+09 ^c , 5.66E+09 ^d , 5.64E+09 ^e
174.1745	128,573.3 ₂ ⁰	- 185,987.0 ₂	3.75E+09	4.10E+09 ^c , 5.39E+09 ^d , 5.43E+09 ^e
174.3831	116,798.2 ₄ ⁰	- 174,143.2 ₃	7.42E+08	1.01E+09 ^c , 1.20E+09 ^d , 1.20E+09 ^e
175.2603	128,929.0 ₃ ⁰	- 185,987.0 ₂	5.11E+08	7.04E+08 ^c , 9.00E+08 ^d , 8.50E+08 ^e
175.9597	117,312.0 ₃ ⁰	- 174,143.2 ₃	4.23E+09	5.55E+09 ^c , 6.97E+09 ^d , 7.13E+09 ^e
177.2082	128,929.0 ₃ ⁰	- 185,359.8 ₄	7.51E+09	8.51E+09 ^c , 1.08E+10 ^d , 1.08E+10 ^e
178.2455	117,312.0 ₃ ⁰	- 173,414.4 ₂	2.89E+09	4.49E+09 ^c , 6.80E+09 ^d , 5.83E+09 ^e
179.7520	128,573.3 ₂ ⁰	- 184,205.5 ₁	2.49E+09	2.79E+09 ^c , 3.45E+09 ^d , 3.45E+09 ^e
199.6179	114,632.8 ₃ ⁰	- 164,728.5 ₄	8.64E+08	8.11E+07 ^c , 8.10E+05 ^d , 1.08E+06 ^e
207.1092	128,573.3 ₂ ⁰	- 176,841.6 ₂	2.58E+08	3.85E+08 ^c , 5.55E+08 ^d , 5.25E+08 ^e
208.5699	116,798.2 ₄ ⁰	- 164,728.5 ₄	1.42E+09	1.78E+09 ^c , 2.33E+09 ^d , 2.32E+09 ^e
208.6470	128,929.0 ₃ ⁰	- 176,841.6 ₂	2.31E+09	2.45E+09 ^c , 3.09E+09 ^d , 3.12E+09 ^e
209.2160	128,573.3 ₂ ⁰	- 176,355.6 ₃	2.38E+09	2.50E+09 ^c , 3.05E+09 ^d , 3.12E+09 ^e
210.4414	116,798.2 ₄ ⁰	- 164,302.3 ₃	3.20E+09	3.43E+09 ^c , 4.27E+09 ^d , 4.29E+09 ^e
210.7853	128,929.0 ₃ ⁰	- 176,355.6 ₃	1.22E+09	1.42E+09 ^c , 1.74E+09 ^d , 1.79E+09 ^e
210.8302	117,312.0 ₃ ⁰	- 164,728.5 ₄	2.22E+09	3.24E+09 ^c
212.7427	117,312.0 ₃ ⁰	- 164,302.3 ₃	2.95E+08	5.18E+08 ^c , 7.07E+08 ^d , 6.85E+08 ^e
219.3745	128,573.3 ₂ ⁰	- 174,143.2 ₃	5.44E+07	8.02E+07 ^c , 1.57E+08 ^d , 9.87E+07 ^e
682.8623	236,667.1 ₅ ⁰	- 251,307.3 ₄	1.21E+07	6.83E+06 ^c
689.0088	248,305.8 ₄ ⁰	- 262,815.4 ₃	7.84E+06	4.59E+06 ^c
704.2842	248,620.5 ₂ ⁰	- 262,815.4 ₃	2.77E+06	6.94E+07 ^c
707.4089	236,667.1 ₅ ⁰	- 250,799.3 ₄	2.75E+06	7.12E+06 ^c
723.2222	236,667.1 ₅ ⁰	- 250,490.3 ₆	5.59E+08	4.38E+08 ^c
730.0030	237,436.9 ₄ ⁰	- 251,131.7 ₅	5.12E+07	2.74E+07 ^c
730.1203	237,106.7 ₃ ⁰	- 250,799.3 ₄	3.85E+06	5.49E+05 ^c
735.4864	237,436.9 ₄ ⁰	- 251,029.6 ₃	2.08E+07	9.65E+06 ^c
735.9575	237,215.3 ₃ ⁰	- 250,799.3 ₄	9.92E+07	1.14E+08 ^c
742.2963	237,663.7 ₆ ⁰	- 251,131.7 ₅	9.03E+06	7.13E+06 ^c
764.1520	237,946.8 ₂ ⁰	- 251,029.6 ₃	9.77E+07	8.71E+07 ^c

Continued

777.3064	249,954.0 ₂ ^o	- 262,815.4 ₃	9.05E+07	5.64E+07 ^c
779.4154	237,663.7 ₆ ^o	- 250,490.3 ₆	7.12E+06	1.01E+07 ^c
791.5103	238,501.1 ₄ ^o	- 251,131.7 ₅	1.89E+08	1.86E+08 ^c
792.4451	249,719.0 ₅ ^o	- 262,334.7 ₆	4.63E+08	3.57E+08 ^c
800.3883	249,682.5 ₃ ^o	- 262,173.0 ₂	2.68E+06	1.63E+06 ^c
812.6327	249,719.0 ₅ ^o	- 262,021.3 ₅	6.85E+06	4.98E+06 ^c
812.9036	238,501.1 ₄ ^o	- 250,799.3 ₄	6.13E+07	1.58E+07 ^c
813.9427	250,789.5 ₄ ^o	- 263,072.0 ₅	2.89E+08	1.76E+08 ^c
818.1726	249,954.0 ₂ ^o	- 262,173.0 ₂	5.96E+07	5.35E+07 ^c
890.0849	250,789.5 ₄ ^o	- 262,021.3 ₅	6.64E+06	2.55E+06 ^c

a: Ritz wavelengths calculated employing the experimental energy level values from [47, 51]. Transitions are given by values (in cm⁻¹) of involved energy levels where subscripts denote their J-values. b: MCDHF values from [38]. pE + q = p.10⁹. c: HFR values from [38]. d: Values from Newton method taken in [36] [37]. e: Values from least-squares method taken in [36] [37].

3.2.2. Ion Hf⁴⁺

As regards Hf V, Sugar and Kaufmann [48] firstly classified 173 lines in the region 545 - 1793 Å and determined 59 energy levels of 4f¹⁴, 4f¹³5d, 4f¹³6s, 4f¹³6p, 4f¹³6d and 4f¹³7s configurations, and secondly [50] classified 5 resonnance transitions 5p⁶-5p⁵ (5d, 6s) in the spectral range 257 - 373 Å. Wyart *et al.* [51] classified 102 lines falling in the domain 459 - 510 Å, established 22 energy levels of the 4f¹³5f configuration.

More recently, we utilized the two theoretical approaches HFR and MCDHF/RCI to produce a set of radiative parameters (transition probabilities and oscillator strengths) for 820 E1 transitions appearing in the region 250 Å - 40 μm [38], 219 of which (about 27%) fulfill reliability criteria (7).

Figure 6 illustrates the comparison between our HFR and MCDHF log gf-values expected reliable, for the strongest lines (log gf > 0), with an average ratio $\langle \text{gf(MCDHF)/gf(HFR)} \rangle$ equal to 0.84 ± 0.20 [38], where we observe an about 15% systematics that could be explained by missing core-valence correlations in our HFR model.

When comparing our MCDHF/RCI and HFR gA-values with respect to the data available in the literature [36] [37], for the strongest lines (gA > 10⁹ s⁻¹), we obtain these average ratios $\langle \text{gA/gA(HFR or MCDHF)} \rangle$: 1.03 ± 0.19 (Newton method set in [36]), 1.03 ± 0.19 (least-squares method set in [36]), 0.89 ± 0.25 (Newton method set in [37]) and 0.87 ± 0.27 (least-squares method set in [37]) with respect to HFR model; 1.34 ± 0.17 (Newton method set in [36]), 1.35 ± 0.17 (least-squares method set in [36]), 0.94 ± 0.11 (Newton method set in [37]) and 0.91 ± 0.19 (least-squares method set in [37]) in respect of our MCDHF/RCI model. Here again, we observe the importance of taking into account the configuration interaction in calculations. **Figure 7** illustrates this effect.

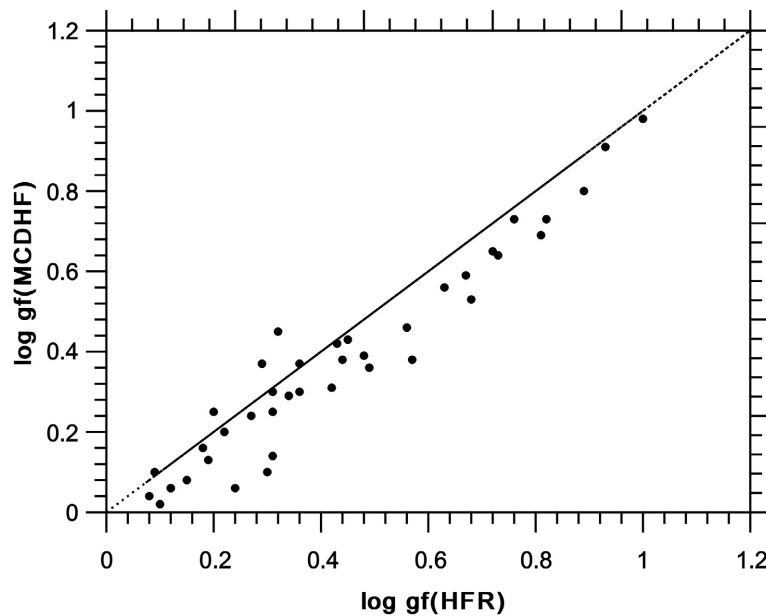
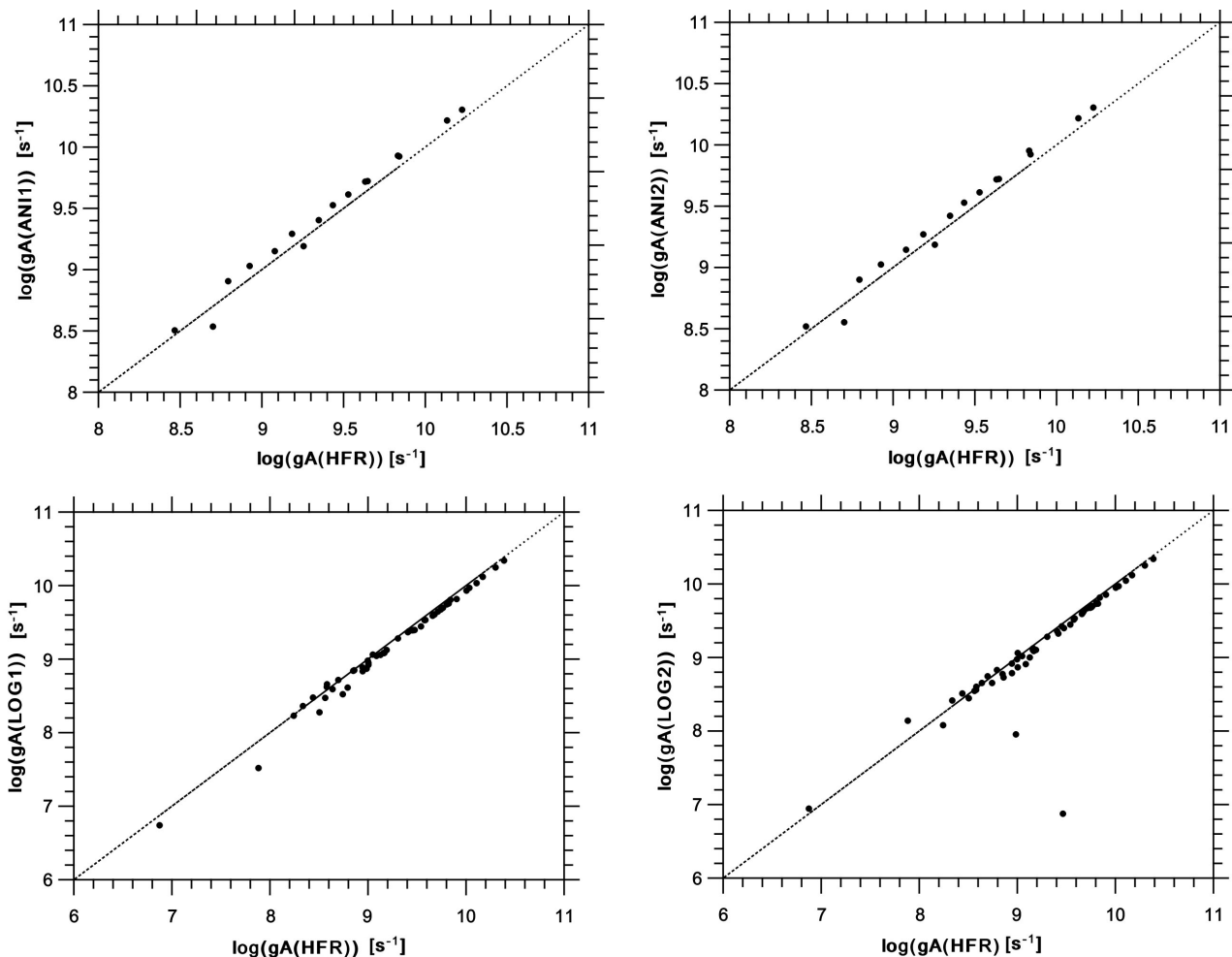


Figure 6. Comparison of our HFR and MCDHF/RCI oscillator strengths ($\log gf$) for Hf V spectral lines [38]. Only transitions with $\log gf > 0$, $CF \geq 0.5$ and $0.9 \leq B/C \leq 1.10$ have been retained.



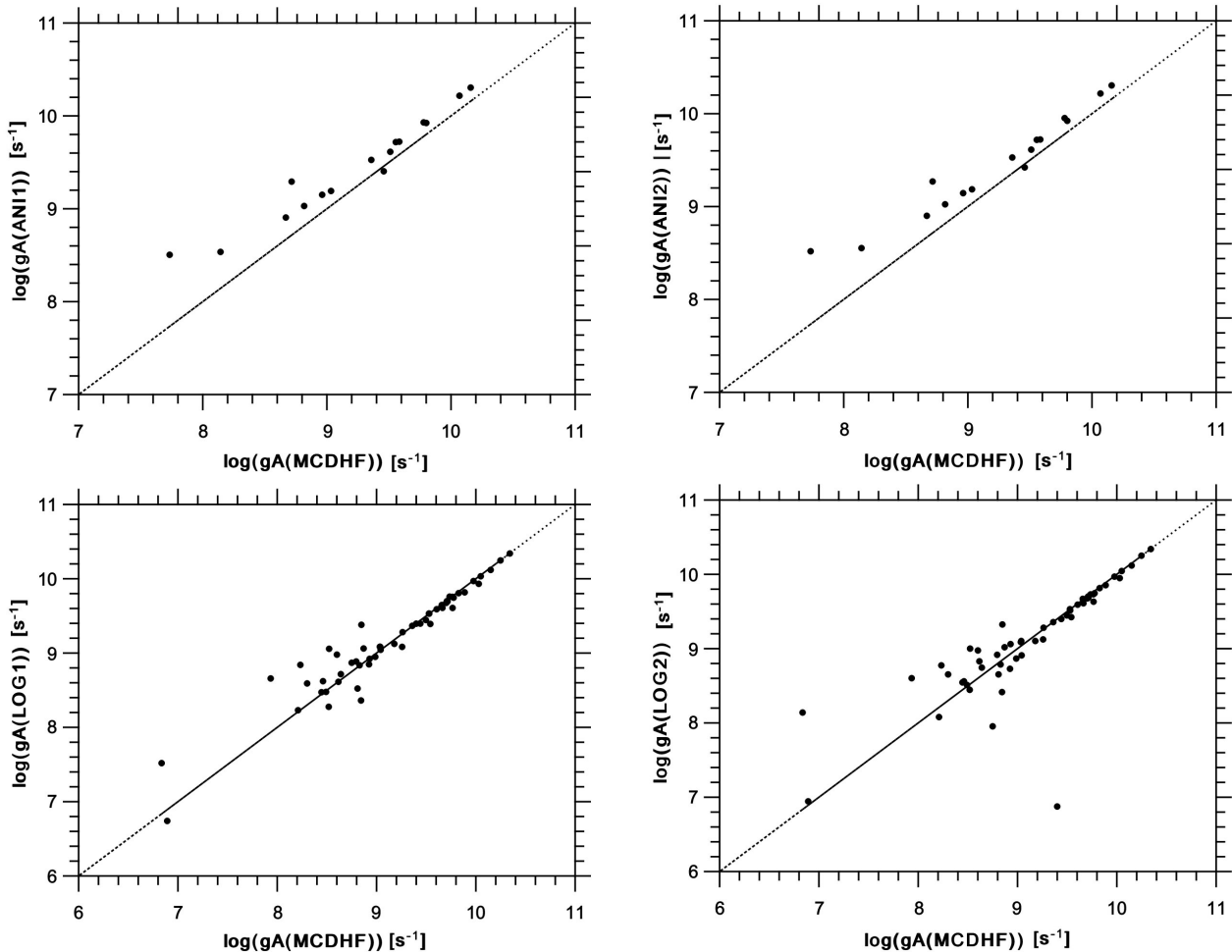


Figure 7. Comparison between our MCDHF/RCI gA-values [38] with the available data [36] [37] for Hf V spectral lines. Only transitions with $\log gf > 00$, CF ≥ 0.5 and $0.9 \leq B/C \leq 1.10$ have been retained.

In the present work, the adopted transition probabilities in Hf^{4+} are the MCDHF data from Bokamba *et al.* [38] which are reported in **Table 5** (column 3) along with other available data (column 4) [36] [37].

3.2.3. Ion Ta^{5+}

Concerning $Ta VI$, Kaufman and Sugar [49] classified 169 lines in the region 218 - 1587 Å and deduced 71 energy levels of $4f^{14}$, $4f^{13}5d$, $4f^{13}6s$, $4f^{13}6p$, $4f^{13}6d$ and $4f^{13}7s$, $5p^55d$, $5p^55d$, $5p^56s$ and $5p^56p$ configurations. Wyart *et al.* [51] classified 96 lines appearing in the range 335 - 409 Å, and determined 26 levels of the $4f^{13}5f$ configuration.

We used the two independent theoretical methods HFR and MCDHF/RCI to determine a set of radiative properties (transition probabilities and oscillator strengths) for 1101 $Ta VI$ allowed spectral lines falling in the range 200 Å - 90 μm [38]. 196 of those E1 transitions (about 22%) satisfy reliability criteria (7).

We compare in **Figure 8** our HFR and MCDHF log gf-values expected reliable, for the strongest lines ($gf > 0$), and we can see that the MCDHF values are almost systematically weaker than the HFR ones. The average ratio $\langle gf(MCDHF)/$

Table 5. Adopted transition probabilities (gA) in Hf V, as well as other available gA-values.

λ (nm) ^a	Transition	Adopted gA (s^{-1}) ^b	Other gA (s^{-1})
45.8280	166,667.05 ₁ - 384,874.4 ₂	8.16E+08	1.38E+09 ^c
45.9847	166,667.05 ₁ - 384,130.7 ₂	5.20E+09	4.97E+09 ^c
46.0721	166,667.05 ₁ - 383,718.1 ₁	1.70E+09	2.35E+09 ^c
46.3085	166,667.05 ₁ - 382,610.0 ₁	6.68E+09	5.88E+09 ^c
47.1355	171,240.86 ₄ - 383,395.3 ₅	1.96E+10	1.83E+10 ^c
47.6577	175,073.22 ₄ - 384,903.0 ₄	1.67E+10	2.21E+10 ^c
47.7817	174,433.1 ₀ - 383,718.1 ₁	8.22E+09	8.92E+09 ^c
48.0026	161,705.88 ₅ - 370,028.1 ₆	1.45E+11	1.89E+11 ^c
48.0026	175,073.22 ₄ - 383,395.3 ₅	1.01E+11	1.40E+11 ^c
48.0361	174,433.1 ₀ - 382,610.0 ₁	8.61E+09	9.88E+09 ^c
48.0385	176,850.41 ₂ - 385,017. ₃	1.71E+10	1.33E+10 ^c
48.1185	176,850.41 ₂ - 384,670.5 ₃	1.86E+10	3.41E+10 ^c
48.2439	176,850.41 ₂ - 384,130.7 ₂	3.52E+09	2.66E+09 ^c
48.4071	164,621.73 ₃ - 371,203.2 ₄	3.37E+10	4.92E+10 ^c
48.6004	176,850.41 ₂ - 382,610.0 ₁	3.76E+09	3.34E+09 ^c
48.7445	166,051.67 ₄ - 371,203.2 ₄	3.89E+10	5.76E+10 ^c
48.8127	166,780.4 ₆ - 371,645.2 ₆	3.14E+10	3.38E+10 ^c
48.8903	166,780.4 ₆ - 371,319.8 ₅	1.85E+09	2.08E+09 ^c
49.0247	181,271.17 ₃ - 385,250.1 ₄	3.89E+09	3.97E+09 ^c
49.0605	181,044.27 ₁ - 384,874.4 ₄	1.26E+10	1.55E+10 ^c
49.0808	181,271.17 ₃ - 385,017. ₃	2.03E+10	1.40E+10 ^c
49.1082	181,271.17 ₃ - 384,903.0 ₄	6.46E+10	8.63E+10 ^c
49.1151	181,271.17 ₃ - 384,874.4 ₂	6.10E+09	8.60E+09 ^c
49.1185	166,780.4 ₆ - 370,369.8 ₇	1.79E+11	2.14E+11 ^c
49.1269	166,667.05 ₁ - 370,221.4 ₁	1.24E+10	1.74E+10 ^c
49.1397	181,867.07 ₅ - 38,5368.7 ₅	2.25E+10	2.47E+10 ^c
49.1644	181,271.17 ₃ - 384,670.5 ₃	1.36E+10	2.90E+10 ^c
49.2011	166,780.4 ₆ - 370,028.1 ₆	2.90E+09	4.58E+09 ^c
49.2401	181,044.27 ₁ - 384,130.7 ₂	1.84E+10	2.03E+10 ^c
49.2524	181,867.07 ₅ - 384,903.0 ₄	7.67E+08	9.79E+08 ^c
49.2952	181,271.17 ₃ - 384,130.7 ₂	3.93E+08	4.24E+08 ^c
49.3404	181,044.27 ₁ - 383,718.1 ₁	1.12E+10	1.54E+10 ^c
49.4248	181,867.07 ₅ - 384,194.6 ₆	1.50E+11	1.81E+11 ^c
49.5648	183,261.02 ₂ - 385,017. ₃	3.49E+10	5.38E+10 ^c
49.6116	181,044.27 ₁ - 382,610.0 ₁	4.92E+09	4.78E+09 ^c

Continued

49.6208	181,867.07 ₅ ^o	- 383,395.3 ₅	2.66E+09	3.80E+09 ^c
49.6210	183,346.90 ₁ ^o	- 384,874.4 ₂	5.46E+09	5.28E+09 ^c
49.6501	183,261.02 ₂ ^o	- 384,670.5 ₃	1.86E+10	8.76E+09 ^c
49.7835	183,261.02 ₂ ^o	- 384,130.7 ₂	2.31E+10	2.83E+10 ^c
49.8048	183,346.90 ₁ ^o	- 384,130.7 ₂	3.73E+09	6.27E+09 ^c
49.8659	171,240.86 ₄ ^o	- 371,778.9 ₄	2.01E+10	3.46E+10 ^c
49.9074	183,346.90 ₁ ^o	- 383,718.1 ₁	6.39E+09	8.03E+09 ^c
50.0974	185,638.77 ₃ ^o	- 385,250.1 ₄	6.61E+10	8.05E+10 ^c
50.1374	172,327.17 ₃ ^o	- 371,778.9 ₄	5.48E+10	7.00E+10 ^c
50.1559	185,638.77 ₃ ^o	- 385,017. ₃	5.73E+09	1.54E+10 ^c
50.1633	183,261.02 ₂ ^o	- 382,610.0 ₁	3.07E+09	3.75E+09 ^c
50.1846	185,638.77 ₃ ^o	- 384,903.0 ₄	1.16E+10	1.23E+10 ^c
50.1849	183,346.90 ₁ ^o	- 382,610.0 ₁	8.22E+09	1.08E+10 ^c
50.1903	171,240.86 ₄ ^o	- 370,482.7 ₃	6.85E+09	7.42E+09 ^c
50.1918	185,638.77 ₃ ^o	- 384,874.4 ₂	5.51E+08	8.87E+08 ^c
50.2189	172,327.17 ₃ ^o	- 371,455.6 ₃	2.48E+10	3.45E+10 ^c
50.2433	185,638.77 ₃ ^o	- 384,670.5 ₃	2.32E+10	1.90E+10 ^c
50.3072	186,590.15 ₄ ^o	- 385,368.7 ₅	1.03E+11	1.24E+11 ^c
50.3373	186,590.15 ₄ ^o	- 385,250.1 ₄	3.06E+10	3.51E+10 ^c
50.3799	185,638.77 ₃ ^o	- 384,130.7 ₂	3.85E+09	4.75E+09 ^c
50.3949	173,212.31 ₅ ^o	- 371,645.2 ₆	1.16E+11	1.42E+11 ^c
50.4254	186,590.15 ₄ ^o	- 384,903.0 ₄	3.73E+09	4.84E+09 ^c
50.4654	172,327.17 ₃ ^o	- 370,482.7 ₄	1.51E+10	1.34E+10 ^c
50.4846	186,590.15 ₄ ^o	- 384,670.5 ₃	4.60E+09	5.99E+09 ^c
50.8117	186,590.15 ₄ ^o	- 383,395.3 ₅	2.17E+09	1.84E+09 ^c
50.9563	175,073.22 ₄ ^o	- 371,319.8 ₅	5.00E+09	4.30E+09 ^c
57.8587	212,533.85 ₄ ^o	- 385,368.7 ₅	1.16E+07	5.06E+06 ^c
58.0150	212,533.85 ₄ ^o	- 384,903.0 ₄	5.44E+05	6.20E+05 ^c
58.0782	213,068.38 ₃ ^o	- 385,250.1 ₄	3.79E+07	2.05E+07 ^c
58.2743	213,068.38 ₃ ^o	- 384,670.5 ₃	1.92E+07	1.27E+07 ^c
58.4582	213,068.38 ₃ ^o	- 384,130.7 ₂	5.23E+06	4.78E+06 ^c
62.9027	226,041.41 ₂ ^o	- 385,017. ₃	2.16E+07	9.90E+06 ^c
62.9779	212,533.85 ₄ ^o	- 371,319.8 ₅	7.26E+06	2.13E+06 ^c
63.1149	226,461.70 ₃ ^o	- 384,903.0 ₄	8.67E+05	1.23E+06 ^c
63.3116	212,533.85 ₄ ^o	- 370,482.7 ₃	6.11E+06	2.88E+06 ^c
76.8520	166,667.05 ₁ ^o	- 296,787.22 ₂	4.37E+08	4.98E+08 ^c , 5.20E+08 ^d , 5.55E+08 ^c

Continued

78.1461	166,667.05 ⁰ ₁	- 296,787.22 ₂	3.10E+08	2.75E+08 ^c , 3.00E+08 ^d , 3.24E+08 ^e
78.6846	156,785.87 ⁰ ₂	- 283,875.57 ₃	1.71E+08	7.07E+08 ^c , 6.93E+08 ^d , 5.95E+08 ^e
80.1299	171,240.86 ⁰ ₄	- 296,038.21 ₄	3.30E+08	3.20E+08 ^c , 1.89E+08 ^d , 2.79E+08 ^e
81.7047	175,073.22 ⁰ ₄	- 297,465.23 ₃	1.09E+09	1.44E+09 ^c , 1.21E+09 ^d , 1.27E+09 ^e
82.6686	175,073.22 ⁰ ₄	- 296,038.21 ₄	7.41E+08	1.12E+09 ^c , 1.15E+09 ^d , 1.04E+09 ^e
82.9086	176,850.41 ⁰ ₂	- 297,465.23 ₃	1.51E+09	1.55E+09 ^c , 1.33E+09 ^d , 1.27E+09 ^e
83.1951	174,433.1 ⁰ ₀	- 294,632.56 ₁	1.83E+09	2.02E+09 ^c , 1.91E+09 ^d , 1.91E+09 ^e
84.9025	176,850.41 ⁰ ₂	- 294,632.56 ₁	1.83E+09	4.35E+08 ^c
85.0796	166,667.05 ⁰ ₁	- 284,204.00 ₂	6.98E+08	2.17E+08 ^c , 2.30E+08 ^d , 2.60E+08 ^e
85.6316	166,051.67 ⁰ ₄	- 282,830.93 ₃	9.71E+08	1.01E+09 ^c , 8.89E+08 ^d , 7.35E+08 ^e
86.0629	181,271.17 ⁰ ₃	- 297,465.23 ₃	1.10E+09	1.22E+09 ^c , 1.11E+09 ^d , 8.12E+08 ^e
86.3091	168,341.35 ⁰ ₂	- 284,204.00 ₂	8.59E+07	3.82E+08 ^c , 4.55E+08 ^d , 4.00E+08 ^e
86.3984	181,044.27 ⁰ ₁	- 296,787.22 ₂	8.40E+08	7.24E+08 ^c , 7.05E+08 ^d , 5.35E+08 ^e
86.5544	168,341.35 ⁰ ₂	- 283,875.57 ₃	3.99E+08	9.94E+08 ^c , 9.52E+08 ^d , 9.45E+08 ^e
86.5681	181,271.17 ⁰ ₃	- 296,787.22 ₂	8.51E+08	1.01E+09 ^c , 8.35E+08 ^d , 1.15E+09 ^e
86.7248	166,780.4 ⁰ ₆	- 282,087.73 ₅	2.20E+10	2.44E+10 ^c , 2.19E+10 ^d , 2.19E+10 ^e
87.1330	181,271.17 ⁰ ₃	- 296,038.21 ₄	6.75E+08	8.82E+08 ^c , 6.84E+08 ^d , 6.12E+08 ^e
87.3442	168,341.35 ⁰ ₂	- 282,830.93 ₃	1.81E+09	1.45E+09 ^c , 1.21E+09 ^d , 1.33E+09 ^e
87.5625	183,261.02 ⁰ ₂	- 297,465.23 ₃	6.24E+08	8.80E+08 ^c , 7.70E+08 ^d , 8.26E+08 ^e
87.5878	181,867.07 ⁰ ₅	- 296,038.21 ₄	1.77E+10	2.00E+10 ^c , 1.76E+10 ^d , 1.78E+10 ^e
87.7401	268,637. ⁰ ₁	- 382,610.0 ₁	8.61E+05	5.11E+08 ^c
87.7872	168,341.35 ⁰ ₂	- 282,253.22 ₂	5.18E+09	5.62E+09 ^c , 4.97E+09 ^d , 5.05E+09 ^e
88.0372	181,044.27 ⁰ ₁	- 294,632.56 ₁	3.39E+09	3.77E+09 ^c , 3.39E+09 ^d , 3.27E+09 ^e
88.0854	183,261.02 ⁰ ₂	- 296,787.22 ₂	5.03E+09	5.53E+09 ^c , 4.74E+09 ^d , 4.75E+09 ^e
88.1521	183,346.90 ⁰ ₁	- 296,787.22 ₂	5.62E+08	9.68E+08 ^c , 7.40E+08 ^d , 9.00E+07 ^e
88.5583	156,785.87 ⁰ ₂	- 296,787.22 ₂	6.71E+09	6.93E+09 ^c , 6.40E+09 ^d , 6.52E+09 ^e
88.5801	171,240.86 ⁰ ₄	- 284,133.06 ₄	5.44E+09	6.35E+09 ^c , 5.74E+09 ^d , 5.36E+09 ^e
89.4243	185,638.77 ⁰ ₃	- 297,465.23 ₃	4.54E+09	5.16E+09 ^c , 4.43E+09 ^d , 4.68E+09 ^e
89.4407	172,327.17 ⁰ ₃	- 284,133.06 ₄	1.08E+09	1.47E+09 ^c , 1.22E+09 ^d , 1.22E+09 ^e
89.6137	171,240.86 ⁰ ₄	- 282,830.93 ₃	7.72E+09	8.02E+09 ^c , 6.56E+09 ^d , 7.14E+09 ^e
89.6472	172,327.17 ⁰ ₃	- 283,875.57 ₃	7.04E+08	2.62E+09 ^c , 2.40E+09 ^d , 2.11E+09 ^e
89.7896	183,261.02 ⁰ ₂	- 294,632.56 ₁	2.29E+09	2.55E+09 ^c , 2.33E+09 ^d , 2.27E+09 ^e
89.8588	183,346.90 ⁰ ₁	- 294,632.56 ₁	6.85E+06	7.64E+07 ^c , 3.30E+07 ^d , 1.38E+08 ^e
89.9698	185,638.77 ⁰ ₃	- 296,787.22 ₂	5.82E+09	6.65E+09 ^c , 5.70E+09 ^d , 5.40E+09 ^e
90.1545	173,212.31 ⁰ ₅	- 284,133.06 ₄	1.12E+10	1.28E+10 ^c , 1.08E+10 ^d , 1.11E+10 ^e
90.1916	186,590.15 ⁰ ₄	- 297,465.23 ₃	9.47E+09	1.08E+10 ^c , 9.31E+09 ^d , 9.31E+09 ^e

Continued

90.2146	171,240.86 ⁰ ₄	- 282,087.73 ₅	2.89E+08	3.80E+08 ^c , 4.18E+08 ^d , 3.63E+08 ^e
90.4947	172,327.17 ⁰ ₃	- 282,830.93 ₃	2.89E+08	3.80E+08 ^c
90.5802	185,638.77 ⁰ ₃	- 296,038.21 ₄	2.79E+08	3.66E+08 ^c , 2.97E+08 ^d , 3.51E+08 ^e
90.9703	172,327.17 ⁰ ₃	- 282,253.22 ₂	2.76E+09	2.99E+09 ^c , 2.49E+09 ^d , 2.51E+09 ^e
91.3675	186,590.15 ⁰ ₄	- 296,038.21 ₄	4.03E+09	4.56E+09 ^c , 3.89E+09 ^d , 3.91E+09 ^e
91.6928	175,073.22 ⁰ ₄	- 284,133.06 ₄	6.44E+08	5.53E+08 ^c , 3.33E+08 ^d , 4.50E+08 ^e
91.8481	173,212.31 ⁰ ₅	- 282,087.73 ₅	5.11E+09	5.82E+09 ^c , 4.99E+09 ^d , 4.97E+09 ^e
91.9098	175,073.22 ⁰ ₄	- 283,875.57 ₃	1.07E+10	1.01E+10 ^c , 8.54E+09 ^d , 8.89E+09 ^e
92.1665	161,705.88 ⁰ ₅	- 270,205.15 ₄	1.41E+10	1.48E+10 ^c , 1.31E+10 ^d , 1.31E+10 ^e
93.1501	176,850.41 ⁰ ₂	- 284,204.00 ₂	4.61E+09	4.66E+09 ^c , 4.06E+09 ^d , 4.08E+09 ^e
93.4453	175,073.22 ⁰ ₄	- 282,087.73 ₅	7.80E+06	7.49E+06 ^c , 5.50E+06 ^d , 8.80E+06 ^e
95.1619	164,621.73 ⁰ ₃	- 269,705.84 ₃	5.97E+09	6.38E+09 ^c , 5.56E+09 ^d , 5.57E+09 ^e
96.0122	166,051.67 ⁰ ₄	- 270,205.15 ₄	5.16E+09	5.70E+09 ^c , 4.92E+09 ^d , 4.82E+09 ^e
96.4747	166,051.67 ⁰ ₄	- 269,705.84 ₃	3.37E+09	3.85E+09 ^c , 3.40E+09 ^d , 3.40E+09 ^e
96.9371	181,044.27 ⁰ ₁	- 284,204.00 ₂	4.13E+08	6.20E+08 ^c , 4.10E+08 ^d , 6.75E+08 ^e
97.1507	181,271.17 ⁰ ₃	- 284,204.00 ₂	3.14E+09	3.47E+09 ^c , 2.79E+09 ^d , 2.80E+09 ^e
97.4617	181,271.17 ⁰ ₃	- 283,875.57 ₃	3.48E+09	2.84E+09 ^c , 2.46E+09 ^d , 2.65E+09 ^e
98.4642	181,271.17 ⁰ ₃	- 282,830.93 ₃	3.33E+08	1.34E+09 ^c , 1.14E+09 ^d , 1.00E+09 ^e
98.8055	181,044.27 ⁰ ₁	- 282,253.22 ₂	1.62E+08	1.75E+08 ^c , 1.70E+08 ^d , 1.20E+08 ^e
99.1502	183,346.90 ⁰ ₁	- 284,204.00 ₂	2.51E+09	2.92E+09 ^c , 2.49E+09 ^d , 7.50E+06 ^e
99.5103	269,705.84 ₃	- 370,198.0 ⁰ ₃	1.08E+09	1.80E+09 ^c , 1.55E+09 ^d , 1.53E+09 ^e
101.1058	183,346.90 ⁰ ₁	- 282,253.22 ₂	7.71E+08	4.78E+08 ^c
105.8544	270,205.15 ₄	- 364,674.5 ⁰ ₃	6.29E+08	3.54E+08 ^c
106.4041	269,705.84 ₃	- 363,687.2 ⁰ ₂	7.38E+08	1.16E+09 ^c
106.6467	282,830.93 ₃	- 376,598.5 ⁰ ₃	1.88E+09	6.29E+09 ^c
107.8425	269,705.84 ₃	- 362,433.7 ⁰ ₃	1.36E+10	2.15E+10 ^c
107.8482	283,875.57 ₃	- 376,598.5 ⁰ ₃	1.01E+10	8.98E+09 ^c
108.4263	270,205.15 ₄	- 362,433.7 ⁰ ₃	3.38E+09	6.12E+09 ^c
109.7280	269,705.84 ₃	- 360,840.3 ⁰ ₂	1.55E+10	2.03E+10 ^c
116.2872	284,204.00 ₂	- 370,198.0 ⁰ ₃	1.39E+08	5.02E+08 ^c , 3.43E+08 ^d , 3.57E+08 ^e
120.8880	282,087.73 ₅	- 364,808.9 ⁰ ₅	1.18E+10	1.22E+10 ^c
121.3279	282,253.22 ₂	- 364,674.5 ⁰ ₃	5.61E+09	5.56E+09 ^c
121.5949	296,038.21 ₄	- 378,278.5 ⁰ ₄	8.80E+09	9.13E+09 ^c
121.7006	294,632.56 ₁	- 376,801.4 ⁰ ₁	7.06E+09	7.54E+09 ^c
121.8977	296,038.21 ₄	- 378,074.2 ⁰ ₃	5.43E+08	6.41E+08 ^c

Continued

122.1843	282,830.93 ₃ - 364,674.5 ₃ ^o	1.03E+10	8.76E+09 ^c
122.4620	282,830.93 ₃ - 364,488.9 ₄ ^o	1.21E+10	9.28E+09 ^c
122.7989	282,253.22 ₂ - 363,687.2 ₂ ^o	1.03E+10	1.02E+10 ^c
123.0209	296,787.22 ₂ - 378,074.2 ₃ ^o	1.15E+10	1.23E+10 ^c
123.2030	282,087.73 ₃ - 363,254.6 ₆ ^o	4.13E+10	4.39E+10 ^c
123.3589	296,038.21 ₄ - 377,102.5 ₅ ^o	3.48E+10	3.70E+10 ^c
123.3991	294,632.56 ₁ - 375,670.4 ₂ ^o	3.34E+08	5.57E+08 ^c
123.6763	282,830.93 ₃ - 363,687.2 ₂ ^o	3.80E+09	2.82E+09 ^c
123.9529	284,133.06 ₄ - 364,808.9 ₅ ^o	2.28E+10	2.47E+10 ^c
124.0490	283,875.57 ₃ - 364,488.9 ₄ ^o	1.94E+09	5.82E+09 ^c
124.1306	296,038.21 ₄ - 376,598.5 ₃ ^o	1.26E+09	1.30E+09 ^c
124.2691	284,204.00 ₄ - 364,674.5 ₃ ^o	1.14E+08	4.61E+08 ^c
124.9345	297,465.23 ₃ - 377,507.2 ₂ ^o	1.03E+09	1.39E+09 ^c
124.9779	296,787.22 ₂ - 376,801.4 ₁ ^o	1.41E+09	1.69E+09 ^c
125.2950	283,875.57 ₃ - 363,687.2 ₁ ^o	7.75E+08	2.08E+09 ^c
125.2956	296,787.22 ₂ - 376,598.5 ₃ ^o	1.77E+09	1.86E+09 ^c
125.5829	282,087.73 ₅ - 361,716.4 ₅ ^o	2.38E+09	2.62E+09 ^c
125.8128	284,204.00 ₂ - 363,687.2 ₂ ^o	2.02E+08	8.93E+08 ^c
126.5371	296,038.21 ₄ - 375,066.4 ₄ ^o	1.93E+09	2.07E+09 ^c
127.1105	284,133.06 ₄ - 362,804.8 ₄ ^o	3.21E+09	3.21E+09 ^c
127.8688	297,465.23 ₃ - 375,670.4 ₂ ^o	2.50E+09	2.35E+09 ^c
128.8640	297,465.23 ₃ - 375,066.4 ₄ ^o	1.85E+09	1.94E+09 ^c
128.8937	284,133.06 ₄ - 361,716.4 ₅ ^o	2.24E+09	2.34E+09 ^c
140.0093	226,041.41 ₂ ^o - 297,465.23 ₃	3.59E+09	4.29E+09 ^c , 5.22E+09 ^d , 5.23E+09 ^e
140.8381	226,461.70 ₃ ^o - 297,465.23 ₃	6.02E+09	6.80E+09 ^c , 8.51E+09 ^d , 8.96E+09 ^e
142.1959	226,461.70 ₃ ^o - 296,787.22 ₂	9.16E+08	1.20E+09 ^c , 1.42E+09 ^d , 1.40E+09 ^e
143.7267	226,461.70 ₃ ^o - 296,038.21 ₄	1.17E+10	1.36E+10 ^c , 1.65E+10 ^d , 1.65E+10 ^e
143.7734	212,533.85 ₄ ^o - 282,087.73 ₅	1.44E+10	1.68E+10 ^c , 2.02E+10 ^d , 2.02E+10 ^e
144.5403	213,068.38 ₃ ^o - 282,253.22 ₂	6.32E+09	6.93E+09 ^c , 8.39E+09 ^d , 8.38E+09 ^e
145.7914	226,041.41 ₂ ^o - 294,632.56 ₁	3.83E+09	4.44E+09 ^c , 5.27E+09 ^d , 5.27E+09 ^e
171.9318	226,041.41 ₂ ^o - 284,204.00 ₂	4.76E+08	6.22E+08 ^c , 8.05E+08 ^d , 7.95E+08 ^e
172.9082	226,041.41 ₂ ^o - 283,875.57 ₃	2.87E+09	2.23E+09 ^c , 2.53E+09 ^d , 2.64E+09 ^e
173.1833	226,461.70 ₃ ^o - 284,204.00 ₂	3.24E+09	3.38E+09 ^c , 4.11E+09 ^d , 4.10E+09 ^e
173.3965	212,533.85 ₄ ^o - 270,205.15 ₄	2.28E+09	2.72E+09 ^c , 3.36E+09 ^d , 3.38E+09 ^e
176.0888	226,041.41 ₂ ^o - 282,830.93 ₃	5.20E+08	1.53E+09 ^c , 1.96E+09 ^d , 1.86E+09 ^e

Continued

176.5616	213,068.38 ₃ ⁰	- 269,705.84 ₃	6.56E+08	8.42E+08 ^c , 1.07E+09 ^d , 1.06E+09 ^e
179.2387	226,461.70 ₃ ⁰	- 282,253.22 ₂	5.41E+07	2.93E+08 ^c , 3.20E+08 ^d , 3.30E+08 ^e
690.7751	370,198.0 ₃ ⁰	- 282,253.22 ₂	4.17E+04	1.54E+05 ^c
818.6751	371,455.6 ₃ ⁰	- 383,667.1 ₃ ⁰	4.01E+03	5.44E+03 ^c
990.4160	361,716.4 ₅ ⁰	- 371,810.4 ₅	1.92E+06	6.18E+05 ^c
1016.3329	375,066.4 ₄ ⁰	- 384,903.0 ₄	2.99E+07	1.65E+07 ^c
1036.8021	360,840.3 ₂ ⁰	- 370,482.7 ₃	1.27E+07	8.99E+06 ^c
1041.0126	361,716.4 ₅ ⁰	- 371,319.8 ₅	3.73E+07	2.03E+07 ^c
1086.1866	375,670.4 ₂ ⁰	- 384,874.4 ₂	3.06E+07	1.88E+07 ^c
1110.7946	375,670.4 ₂ ⁰	- 384,670.5 ₃	1.91E+07	1.46E+07 ^c
1140.0037	362,433.7 ₃ ⁰	- 371,203.2 ₄	2.93E+07	2.01E+07 ^c
1155.5392	376,598.5 ₃ ⁰	- 385,250.1 ₄	3.35E+06	1.42E+06 ^c
1191.4838	363,254.6 ₆ ⁰	- 371,645.2 ₆	2.79E+07	1.43E+07 ^c
1203.8370	376,598.5 ₃ ⁰	- 384,903.0 ₄	6.01E+07	3.18E+07 ^c
1209.4147	377,102.5 ₅ ⁰	- 385,368.7 ₅	1.94E+07	9.94E+06 ^c
1238.3581	376,801.4 ₁ ⁰	- 384,874.4 ₂	1.00E+07	4.26E+06 ^c
1239.5557	363,254.6 ₆ ⁰	- 371,319.8 ₅	1.54E+06	6.73E+05 ^c
1242.0505	362,433.7 ₃ ⁰	- 370,482.7 ₃	2.52E+07	1.54E+07 ^c
1286.9143	363,687.2 ₂ ⁰	- 371,455.6 ₃	2.08E+07	1.12E+07 ^c
1331.2293	377,507.2 ₂ ⁰	- 385,017. ₃	2.33E+07	1.46E+07 ^c
1364.0138	376,801.4 ₁ ⁰	- 384,130.7 ₂	1.07E+07	5.95E+06 ^c
1365.4670	364,488.9 ₄ ⁰	- 371,810.4 ₅	5.10E+07	2.56E+07 ^c
1395.6231	377,507.2 ₂ ⁰	- 384,670.5 ₃	9.84E+06	1.84E+06 ^c
1407.1937	364,674.5 ₃ ⁰	- 371,778.9 ₄	2.83E+07	1.72E+07 ^c
1445.3811	376,801.4 ₁ ⁰	- 383,718.1 ₁	5.76E+06	2.32E+06 ^c
1462.3799	364,808.9 ₅ ⁰	- 371,645.2 ₆	6.40E+07	3.16E+07 ^c
1463.5359	364,488.9 ₄ ⁰	- 371,319.8 ₅	3.01E+06	1.78E+06 ^c
1471.1600	363,687.2 ₂ ⁰	- 370,482.7 ₃	2.19E+06	2.82E+05 ^c
1488.9516	364,488.9 ₄ ⁰	- 371,203.2 ₄	9.94E+06	2.41E+06 ^c
1509.3633	377,507.2 ₂ ⁰	- 384,130.7 ₂	9.98E+06	5.16E+06 ^c
1535.4664	364,808.9 ₅ ⁰	- 371,319.8 ₅	5.15E+06	1.81E+06 ^c
1721.2337	364,674.5 ₃ ⁰	- 370,482.7 ₃	3.95E+06	1.68E+06 ^c

^aRitz wavelengths calculated employing the experimental energy level values. Transitions are given by values (in cm^{-1}) of involved energy levels where subscripts denote their J-values. b: MCDHF values from [38]. pE + q = p. 10^q . c: HFR values from [38]. d: Values from Newton method taken in [36] [37]. e: Values from least-squares method taken in [36] [37].

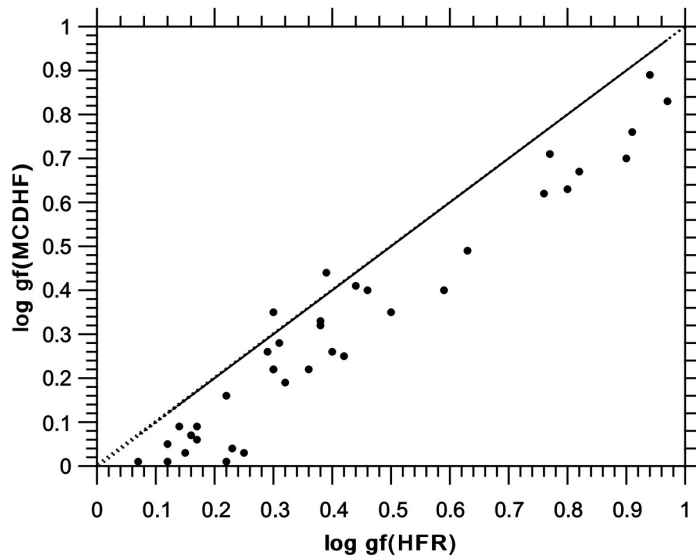


Figure 8. Comparison of our HFR and MCDHF/RCI oscillator strengths ($\log gf$) for Ta VI spectral lines [38]. Only transitions with $\log gf > 0$, $CF \geq 0.5$ and $0.9 \leq B/C \leq 1.10$ have been retained.

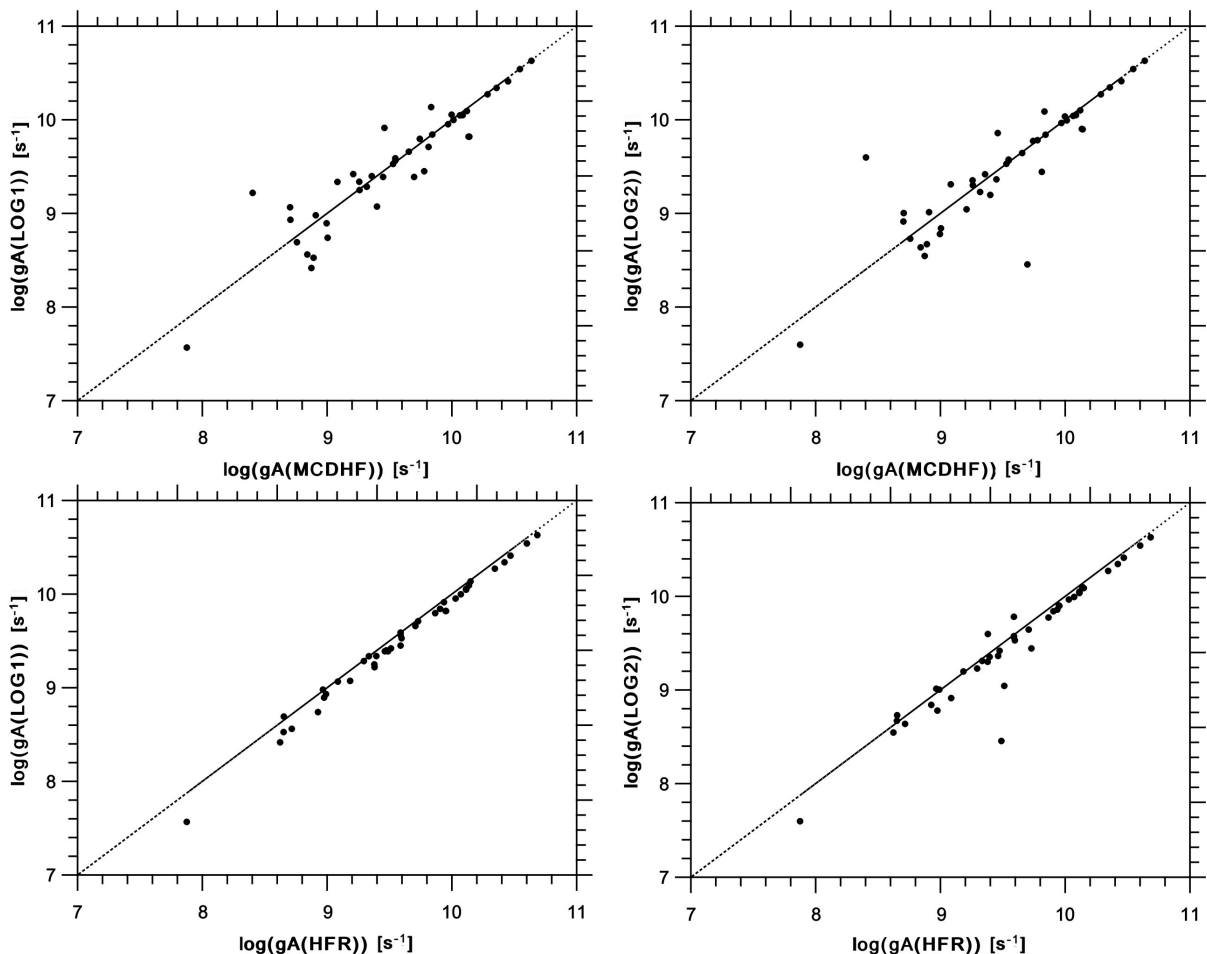


Figure 9. Comparison between our MCDHF/RCI and HFR gA-values [38] with those published by Loginov and Tuchkin [37] for Ta VI spectral lines. Only transitions with $\log gf > 0$, $CF \geq 0.5$ and $0.9 \leq B/C \leq 1.10$ have been retained.

$\langle gf(HFR) \rangle$ being equal to 0.75 ± 0.18 , the observed systematics is thus about 25% and this trend is probably caused by missing interactions with configurations having two holes in the 5p subshell in our HFR model.

The comparison between our MCDHF/RCI and HFR gA-values with the data by [37], for the strongest lines ($gA > 10^9 \text{ s}^{-1}$), gives these average ratios $\langle gA/gA (\text{HFR or MCDHF}) \rangle$: 0.94 ± 0.55 (Newton method set in [37]) and 1.01 ± 1.11 (least-squares method set in [37]) with respect to HFR model; 0.97 ± 0.49 (Newton method set in [37]) and 0.92 ± 0.45 (least-squares method set in [37]) in respect of our MCDHF/RCI model. We observe a similar trend of the effects of configuration interaction on the gA-values as in the cases of Lu IV and Hf V, which is shown in Figure 9.

In the present work, the adopted transition probabilities in Ta^{5+} are the MCDHF data from Bokamba *et al.* [38] which are reported in Table 6 (column 3) along with other available data (column 4) [37].

Table 6. Adopted transition probabilities (gA) in Ta VI, as well as other available gA-values.

λ (nm) ^a	Transition	Adopted gA (s^{-1}) ^b	Other gA (s^{-1})
21.8259	$0.0_0 - 458,172.0_1^o$	1.43E+10	7.38E+10 ^c
26.0048	$0.0_0 - 384,545.2_1^o$	6.28E+10	5.16E+10 ^c
37.3512	$242,614.2_1^o - 510,343.0_1$	1.09E+10	1.50E+10 ^c
37.5722	$230,924.4_2^o - 497,079.0_3$	2.27E+10	3.50E+10 ^c
37.7279	$230,924.4_2^o - 495,980.0_2$	5.01E+10	7.84E+10 ^c
38.1708	$251,742.8_4^o - 513,723.0_4$	2.33E+10	4.19E+10 ^c
38.3359	$242,614.2_1^o - 503,466.0_0$	1.61E+10	2.57E+10 ^c
38.4766	$253,591.0_2^o - 513,489.0_2$	4.93E+10	8.08E+10 ^c
38.4840	$236,438.8_5^o - 496,287.0_6$	2.32E+11	3.60E+11 ^c
38.5888	$239,599.4_3^o - 498,742.0_2$	4.20E+09	5.49E+09 ^c
38.6792	$251,806.0_0^o - 510,343.0_1$	1.09E+10	1.40E+10 ^c
38.9012	$241,235.5_4^o - 498,297.0_3$	5.99E+09	6.25E+09 ^c
39.0045	$239,599.4_3^o - 495,980.0_2$	3.25E+10	5.20E+10 ^c
39.0430	$242,614.2_1^o - 498,742.0_2$	1.54E+10	2.30E+10 ^c
39.0864	$241,235.5_4^o - 497,079.0_3$	1.51E+10	2.73E+10 ^c
39.1394	$243,309.0_6^o - 498,806.0_6$	5.13E+10	6.47E+10 ^c
39.1998	$258,566.4_3^o - 513,670.0_6$	2.12E+10	1.59E+10 ^c
39.2400	$243,309.0_6^o - 498,151.0_5$	3.18E+09	4.01E+09 ^c
39.2757	$258,566.4_3^o - 513,177.0_5$	3.34E+10	6.43E+10 ^c
39.3855	$260,457.1_5^o - 514,358.0_5$	3.70E+10	4.75E+10 ^c
39.4454	$243,309.0_6^o - 496,824.0_7$	2.94E+11	4.05E+11 ^c
39.4842	$260,457.1_5^o - 513,723.0_4$	1.47E+09	1.70E+09 ^c
39.5291	$243,309.0_6^o - 496,287.0_6$	5.34E+09	9.68E+09 ^c

Continued

39.5554	258,774.2 ₁ ^o	- 511,584.0 ₁	2.32E+10	4.18E+10 ^c
39.6630	260,457.1 ₅ ^o	- 512,581.0 ₆	2.48E+11	3.43E+11 ^c
39.7347	244,923.7 ₂ ^o	- 496,593.0 ₁	1.73E+10	2.53E+10 ^c
39.8189	260,457.1 ₅ ^o	- 511,594.0 ₅	4.63E+09	7.63E+09 ^c
39.8716	248,055.0 ₄ ^o	- 498,860.0 ₅	1.08E+11	1.63E+11 ^c
39.9608	260,097.8 ₁ ^o	- 510,343.0 ₁	1.75E+10	3.36E+10 ^c
39.9847	248,055.0 ₄ ^o	- 498,151.0 ₅	3.91E+09	1.33E+10 ^c
40.1029	249,484.5 ₅ ^o	- 498,843.0 ₄	9.46E+10	1.31E+11 ^c
40.1400	264,541.9 ₃ ^o	- 513,670.0 ₃	1.88E+10	3.91E+10 ^c
40.1692	264,541.9 ₃ ^o	- 513,489.0 ₂	1.15E+09	4.08E+09 ^c
40.1909	249,484.5 ₃ ^o	- 498,297.0 ₃	4.56E+10	6.92E+10 ^c
40.2204	265,728.2 ₄ ^o	- 514,358.0 ₅	1.73E+11	2.35E+11 ^c
40.2585	261,948.0 ₂ ^o	- 510,343.0 ₁	5.05E+09	7.97E+09 ^c
40.2788	250,536.4 ₅ ^o	- 498,806.0 ₆	1.95E+11	2.70E+11 ^c
40.3031	264,541.9 ₃ ^o	- 512,662.0 ₂	6.08E+09	7.01E+09 ^c
40.4666	251,742.8 ₄ ^o	- 498,860.0 ₅	3.71E+10	2.74E+10 ^c
40.5687	249,484.5 ₃ ^o	- 495,980.0 ₂	6.29E+09	8.98E+09 ^c
40.7604	251,742.8 ₄ ^o	- 497,079.0 ₃	1.34E+09	7.56E+08 ^c
40.8677	258,774.2 ₁ ^o	- 503,466.0 ₀	1.13E+09	1.64E+09 ^c
43.1166	230,924.4 ₂ ^o	- 462,853.7 ₃	3.94E+07	5.31E+07 ^c
44.9425	244,923.7 ₂ ^o	- 467,430.1 ₂	2.65E+07	2.27E+07 ^c
45.1227	241,235.5 ₄ ^o	- 462,853.7 ₃	2.69E+08	3.60E+08 ^c
45.7639	244,923.7 ₂ ^o	- 463,436.4 ₁	2.80E+08	3.00E+08 ^c
45.8863	244,923.7 ₂ ^o	- 462,853.7 ₃	1.86E+07	1.22E+07 ^c
46.5552	248,055.0 ₄ ^o	- 462,853.7 ₃	3.27E+08	4.68E+08 ^c
46.8671	249,484.5 ₃ ^o	- 462,853.7 ₃	1.43E+08	1.34E+08 ^c
47.3685	251,742.8 ₄ ^o	- 462,853.7 ₃	4.49E+07	2.68E+07 ^c
47.9258	258,774.2 ₁ ^o	- 467,430.1 ₂	2.40E+05	4.68E+06 ^c
48.1498	306,511.8 ₃ ^o	- 514,197.0 ₄	2.42E+08	6.98E+08 ^c
48.8610	258,774.2 ₁ ^o	- 463,436.4 ₁	1.91E+07	1.90E+08 ^c
49.2238	242,614.2 ₁ ^o	- 445,767.9 ₁	2.16E+08	2.10E+08 ^c
49.7746	261,948.0 ₂ ^o	- 462,853.7 ₃	1.35E+07	1.54E+07 ^c
49.9994	296,590.5 ₁ ^o	- 496,593.0 ₁	9.00E+07	1.80E+08 ^c
50.7291	265,728.2 ₄ ^o	- 462,853.7 ₃	5.16E+07	8.15E+07 ^c
51.5461	320,195.9 ₃ ^o	- 514,197.0 ₄	1.04E+08	2.52E+07 ^c
51.5565	251,806.0 ₀ ^o	- 445,767.9 ₁	1.32E+08	1.42E+08 ^c
56.0043	335,112.2 ₂ ^o	- 513,670.0 ₃	3.39E+07	1.04E+07 ^c

Continued

56.5791	242,614.2 ₁ ^o	- 419,358.0 ₂	8.11E+08	9.26E+08 ^c , 9.55E+08 ^d , 1.03E+09 ^e
57.3954	242,614.2 ₁ ^o	- 416,844.3 ₁	5.73E+08	4.50E+08 ^c , 4.92E+08 ^d , 5.37E+08 ^e
58.5344	296,590.5 ₁ ^o	- 467,430.1 ₂	1.54E+09	1.63E+09 ^c
58.6656	248,055.0 ₄ ^o	- 418,512.6 ₄	1.01E+09	8.45E+08 ^c , 5.49E+08 ^d , 6.93E+08 ^e
59.9629	251,742.8 ₄ ^o	- 418,512.6 ₄	1.21E+09	2.16E+09 ^c , 2.17E+09 ^d , 2.04E+09 ^e
60.0311	253,591.0 ₂ ^o	- 420,171.3 ₃	2.81E+09	2.90E+09 ^c , 2.45E+09 ^d , 2.31E+09 ^e
60.4561	239,599.4 ₃ ^o	- 405,008.8 ₄	4.37E+09	4.66E+09 ^c , 3.88E+09 ^d , 3.75E+09 ^e
60.5920	251,806.0 ₀ ^o	- 416,844.3 ₁	3.52E+09	3.88E+09 ^c , 3.66E+09 ^d , 3.66E+09 ^e
61.2545	253,591.0 ₂ ^o	- 416,844.3 ₁	5.08E+08	9.80E+08 ^c , 8.55E+08 ^d , 1.01E+09 ^e
61.3745	241,235.5 ₄ ^o	- 404,169.7 ₃	5.05E+08	1.22E+09 ^c , 1.16E+09 ^d , 8.19E+08 ^e
61.8793	258,566.4 ₃ ^o	- 420,171.3 ₃	2.08E+09	1.97E+09 ^c , 1.93E+09 ^d , 1.69E+09 ^e
61.9652	241,235.5 ₄ ^o	- 402,616.4 ₅	1.81E+09	2.48E+09 ^c , 2.18E+09 ^d , 2.26E+09 ^e
62.1923	258,566.4 ₃ ^o	- 419,358.0 ₂	1.82E+09	2.39E+09 ^c , 1.78E+09 ^d , 2.00E+09 ^e
62.7717	243,309.0 ₆ ^o	- 402,616.4 ₅	4.34E+10	4.84E+10 ^c , 4.27E+10 ^d , 4.27E+10 ^e
62.7903	260,097.8 ₁ ^o	- 419,358.0 ₂	1.62E+09	3.25E+09 ^c , 2.63E+09 ^d , 1.11E+09 ^e
63.2631	258,774.2 ₁ ^o	- 416,844.3 ₁	6.50E+09	5.36E+09 ^c , 5.13E+09 ^d , 2.78E+09 ^e
63.2689	260,457.1 ₅ ^o	- 418,512.6 ₄	3.51E+10	3.99E+10 ^c , 3.47E+10 ^d , 3.48E+10 ^e
63.7000	306,450.5 ₂ ^o	- 463,436.4 ₁	1.21E+09	1.05E+09 ^c
63.7741	244,923.7 ₂ ^o	- 401,727.1 ₃	7.79E+08	4.48E+08 ^c , 3.36E+08 ^d , 4.69E+08 ^e
63.7973	260,097.8 ₁ ^o	- 416,844.3 ₁	2.53E+08	2.40E+09 ^c , 1.66E+09 ^d , 3.96E+09 ^e
63.9373	306,450.5 ₂ ^o	- 462,853.7 ₃	2.21E+09	2.41E+09 ^c
64.0555	248,055.0 ₄ ^o	- 404,169.7 ₃	2.88E+09	8.64E+09 ^c , 8.19E+09 ^d , 7.21E+09 ^e
64.2552	264,541.9 ₃ ^o	- 420,171.3 ₃	9.32E+09	1.07E+10 ^c , 8.96E+09 ^d , 9.24E+09 ^e
64.2986	249,484.5 ₃ ^o	- 405,008.8 ₄	2.28E+09	2.98E+09 ^c , 2.50E+09 ^d , 2.62E+09 ^e
64.3585	230,924.4 ₂ ^o	- 386,304.1 ₃	1.32E+10	1.37E+10 ^c , 1.24E+10 ^d , 1.26E+10 ^e
64.5168	307,855.3 ₄ ^o	- 462,853.7 ₃	2.45E+10	3.35E+10 ^c
64.5593	261,948.0 ₂ ^o	- 416,844.3 ₁	4.52E+09	5.10E+09 ^c , 4.56E+09 ^d , 4.41E+09 ^e
64.5928	264,541.9 ₃ ^o	- 419,358.0 ₂	1.16E+10	1.30E+10 ^c , 1.12E+10 ^d , 1.10E+10 ^e
64.6474	249,484.5 ₃ ^o	- 404,169.7 ₃	9.95E+09	1.30E+10 ^c , 1.13E+10 ^d , 1.09E+10 ^e
64.7365	250,536.4 ₅ ^o	- 405,008.8 ₄	2.28E+10	2.64E+10 ^c , 2.19E+10 ^d , 2.21E+10 ^e
64.7488	265,728.2 ₄ ^o	- 420,171.3 ₃	1.93E+10	2.21E+10 ^c , 1.87E+10 ^d , 1.87E+10 ^e
65.0736	248,055.0 ₄ ^o	- 401,727.1 ₃	1.36E+10	8.91E+09 ^c , 6.60E+09 ^d , 7.98E+09 ^e
65.4433	345,938.0 ₁ ^o	- 498,742.0 ₂	6.73E+07	9.34E+07 ^c
65.4865	249,484.5 ₃ ^o	- 402,187.7 ₂	4.98E+09	3.08E+09 ^c , 2.45E+09 ^d , 2.85E+08 ^e
65.6052	251,742.8 ₄ ^o	- 404,169.7 ₃	1.38E+10	8.98E+09 ^c , 6.60E+09 ^d , 7.91E+09 ^e
65.7549	250,536.4 ₅ ^o	- 402,616.4 ₅	1.03E+10	1.18E+10 ^c , 9.96E+09 ^d , 9.85E+09 ^e
65.9853	296,590.5 ₁ ^o	- 448,139.5 ₂	1.49E+09	1.53E+09 ^c

Continued

66.4105	253,591.0 ₂ ^o	- 404,169.7 ₃	6.94E+08	5.21E+08 ^c , 3.64E+08 ^d , 4.34E+08 ^e
66.4699	236,438.8 ₆ ^o	- 386,882.9 ₄	2.82E+10	2.95E+10 ^c , 2.57E+10 ^d , 2.58E+10 ^e
66.5689	313,216.2 ₂ ^o	- 463,436.4 ₁	9.77E+09	1.19E+10 ^c
66.6737	251,742.8 ₄ ^o	- 401,727.1 ₃	6.82E+09	1.41E+10 ^c , 1.37E+10 ^d , 1.23E+10 ^e
67.0343	296,590.5 ₁ ^o	- 445,767.9 ₁	5.98E+09	6.78E+09 ^c
67.8963	239,599.4 ₃ ^o	- 386,882.9 ₄	3.38E+09	3.95E+09 ^c , 3.38E+09 ^d , 3.38E+09 ^e
68.1641	239,599.4 ₃ ^o	- 386,304.1 ₃	1.22E+10	1.30E+10 ^c , 1.12E+10 ^d , 1.12E+10 ^e
68.2862	258,566.4 ₃ ^o	- 405,008.8 ₄	7.51E+07	7.50E+07 ^c , 3.69E+07 ^d , 3.96E+07 ^e
68.6798	258,566.4 ₃ ^o	- 404,169.7 ₃	2.51E+09	1.53E+09 ^c , 1.18E+09 ^d , 1.58E+09 ^e
68.9329	241,235.5 ₄ ^o	- 386,304.1 ₃	6.96E+09	8.04E+09 ^c , 6.95E+09 ^d , 6.92E+09 ^e
69.0376	258,566.4 ₃ ^o	- 403,415.0 ₂	6.00E+09	3.88E+09 ^c , 2.82E+09 ^d , 6.05E+09 ^e
69.3740	323,283.8 ₃ ^o	- 467,430.1 ₂	1.39E+10	1.62E+10 ^c
69.8516	258,566.4 ₃ ^o	- 401,727.1 ₃	5.53E+09	7.35E+09 ^c , 6.26E+09 ^d , 5.94E+09 ^e
69.9285	319,850.5 ₄ ^o	- 462,853.7 ₃	4.30E+09	7.79E+08 ^c
70.7312	244,923.7 ₂ ^o	- 386,304.1 ₃	9.91E+08	9.46E+08 ^c , 7.84E+08 ^d , 6.02E+08 ^e
71.7785	306,450.5 ₂ ^o	- 445,767.9 ₁	4.47E+09	5.26E+09 ^c
73.9973	251,742.8 ₄ ^o	- 386,882.9 ₄	7.48E+08	4.20E+08 ^c , 2.61E+08 ^d , 3.51E+08 ^e
74.1162	313,216.2 ₂ ^o	- 448,139.5 ₂	2.67E+09	2.66E+09 ^c
75.8874	335,655.9 ₃ ^o	- 467,430.1 ₂	1.73E+09	1.03E+08 ^c
76.6224	401,727.1 ₃ ^o	- 532,237.2 ₃ ^o	4.35E+09	7.30E+09 ^c
76.7134	386,304.1 ₃ ^o	- 516,659.5 ₄ ^o	1.39E+10	1.66E+10 ^c
76.7311	401,727.1 ₃ ^o	- 532,052.4 ₂ ^o	8.50E+09	1.16E+10 ^c
76.8938	402,187.7 ₂ ^o	- 532,237.2 ₃ ^o	2.03E+09	7.96E+09 ^c
76.9532	386,882.9 ₄ ^o	- 516,832.1 ₃ ^o	1.25E+10	1.48E+10 ^c
77.0555	386,882.9 ₄ ^o	- 516,659.5 ₄ ^o	5.80E+09	8.96E+09 ^c
77.6264	403,415.0 ₂ ^o	- 532,237.2 ₃ ^o	7.63E+09	4.08E+09 ^c
78.1967	404,169.7 ₃ ^o	- 532,052.4 ₂ ^o	1.80E+09	9.29E+08 ^c
85.1075	345,938.0 ₁ ^o	- 463,436.4 ₁	1.63E+09	1.51E+09 ^c
86.7995	416,844.3 ₁ ^o	- 532,052.4 ₂ ^o	7.21E+09	6.05E+09 ^c
86.8101	386,882.9 ₄ ^o	- 502,076.9 ₃ ^o	5.31E+08	4.94E+08 ^c
87.2262	402,187.7 ₂ ^o	- 516,832.1 ₃ ^o	8.42E+09	3.20E+09 ^c
87.6862	402,616.4 ₃ ^o	- 516,659.5 ₄ ^o	2.41E+10	2.11E+10 ^c
87.9317	418,512.6 ₄ ^o	- 532,237.2 ₃ ^o	1.93E+10	1.72E+10 ^c
87.9347	306,450.5 ₂ ^o	- 420,171.3 ₃	1.31E+06	3.11E+06 ^c
87.9821	306,511.8 ₃ ^o	- 420,171.3 ₃	3.07E+07	5.66E+07 ^c
88.0655	401,727.1 ₃ ^o	- 515,279.0 ₃ ^o	1.51E+10	2.24E+10 ^c
88.1701	403,415.0 ₂ ^o	- 516,832.1 ₃ ^o	1.32E+09	4.91E+09 ^c

Continued

88.2924	386,304.1 ₃ - 499,564.2 ₄ ^o	1.55E+10	2.16E+10 ^c
88.5681	306,450.5 ₂ ^o - 419,358.0 ₄	7.50E+06	1.52E+07 ^c
88.5903	419,358.0 ₂ - 532,237.2 ₃ ^o	1.70E+09	1.48E+09 ^c
88.7356	419,358.0 ₂ - 532,052.4 ₂ ^o	8.07E+09	7.69E+09 ^c
88.8970	404,169.7 ₃ - 516,659.5 ₄ ^o	2.02E+09	1.99E+09 ^c
89.0345	307,855.3 ₄ ^o - 420,171.3 ₃	1.49E+07	1.28E+07 ^c
89.1271	386,882.9 ₄ ^o - 499,082.2 ₃	6.71E+09	9.69E+09 ^c
89.3806	420,171.3 ₃ - 532,052.4 ₂ ^o	5.22E+09	4.90E+09 ^c
89.3943	403,415.0 ₂ - 515,279.0 ₃ ^o	1.19E+10	7.88E+09 ^c
89.4268	405,008.8 ₄ - 516,832.1 ₃ ^o	5.94E+09	5.44E+09 ^c
89.5062	401,727.1 ₃ - 513,451.2 ₄ ^o	3.50E+10	5.29E+10 ^c
90.0015	404,169.7 ₃ - 515,279.0 ₃ ^o	2.70E+09	1.60E+09 ^c
90.3691	307,855.3 ₄ ^o - 418,512.6 ₄	1.74E+07	1.53E+07 ^c
91.5068	404,169.7 ₃ - 513,451.2 ₄ ^o	8.78E+09	4.89E+09 ^c
100.2938	402,616.4 ₅ - 502,323.5 ₅ ^o	1.70E+10	1.83E+10 ^c
100.7982	401,727.1 ₃ - 500,935.2 ₂ ^o	1.10E+09	5.54E+08 ^c
100.8529	418,512.6 ₄ - 517,666.9 ₄ ^o	1.23E+10	1.34E+10 ^c
101.5259	306,511.8 ₃ ^o - 405,008.8 ₄	7.93E+08	1.78E+08 ^c
102.2083	402,616.4 ₅ - 500,455.8 ₆ ^o	5.84E+10	6.63E+10 ^c
102.3234	418,512.6 ₄ - 516,242.0 ₅ ^o	4.91E+10	5.59E+10 ^c
102.3983	306,511.8 ₃ ^o - 404,169.7 ₃	1.11E+09	2.49E+08 ^c
102.7585	419,358.0 ₂ - 516,673.6 ₂ ^o	1.33E+10	1.51E+10 ^c
102.7594	405,008.8 ₄ - 502,323.5 ₅ ^o	3.20E+10	3.76E+10 ^c
103.0205	405,008.8 ₄ - 502,076.9 ₃ ^o	3.11E+09	3.96E+09 ^c
103.3417	418,512.6 ₄ - 515,279.0 ₃ ^o	1.75E+09	1.89E+09 ^c
103.3426	404,169.7 ₃ - 500,935.2 ₂ ^o	5.10E+09	7.12E+09 ^c
103.8266	307,855.3 ₄ ^o - 404,169.7 ₃	2.06E+08	2.15E+07 ^c
104.5471	402,616.4 ₅ - 498,267.1 ₅ ^o	3.40E+09	4.12E+09 ^c
105.0103	323,283.8 ₃ ^o - 418,512.6 ₄	2.12E+09	2.03E+08 ^c
105.0251	306,511.8 ₃ ^o - 401,727.1 ₃	2.60E+08	2.92E+07 ^c
105.3312	418,512.6 ₄ - 513,451.2 ₄ ^o	2.72E+09	3.29E+09 ^c
105.5285	307,855.3 ₄ ^o - 402,616.4 ₅	2.83E+09	2.98E+08 ^c
106.3000	405,008.8 ₄ - 499,082.2 ₃ ^o	4.90E+09	5.25E+09 ^c
106.4240	420,171.3 ₃ - 514,135.1 ₂ ^o	3.22E+09	3.45E+09 ^c
107.2042	420,171.3 ₃ - 513,451.2 ₄ ^o	2.53E+09	2.77E+09 ^c
107.2291	405,008.8 ₄ - 513,451.2 ₄ ^o	3.08E+09	3.39E+09 ^c
114.9487	380,434.8 ₂ - 467,430.1 ₂ ^o	6.70E+08	5.69E+09 ^c

Continued

117.5653	335,112.2 ₂ ^o	- 420,171.3 ₃	5.02E+09	6.34E+09 ^c
117.9066	320,195.9 ₃ ^o	- 405,008.8 ₄	5.17E+09	6.80E+09 ^c
118.5970	319,850.5 ₄ ^o	- 404,169.7 ₃	1.45E+09	2.53E+09 ^c
118.7003	335,112.2 ₂ ^o	- 419,358.0 ₂	7.93E+09	9.44E+09 ^c
119.0848	320,195.9 ₃ ^o	- 404,169.7 ₃	7.90E+09	1.09E+10 ^c
120.6492	384,545.2 ₁ ^o	- 467,430.1 ₂	3.71E+09	5.59E+09 ^c
120.6903	335,655.9 ₃ ^o	- 418,512.6 ₄	1.41E+10	1.97E+10 ^c
122.1350	319,850.5 ₄ ^o	- 401,727.1 ₃	2.88E+08	1.77E+08 ^c
122.3510	335,112.2 ₂ ^o	- 416,844.3 ₁	5.22E+09	6.43E+09 ^c
122.6524	320,195.9 ₃ ^o	- 401,727.1 ₃	1.76E+09	8.38E+08 ^c
124.4228	306,511.8 ₃ ^o	- 386,882.9 ₄	6.61E+08	9.22E+07 ^c
124.7953	323,283.8 ₃ ^o	- 403,415.0 ₂	3.78E+08	3.74E+08 ^c
126.7365	323,283.8 ₃ ^o	- 402,187.7 ₂	2.06E+08	5.71E+08 ^c
127.4717	307,855.3 ₄ ^o	- 386,304.1 ₃	8.60E+08	1.10E+08 ^c
127.4806	323,283.8 ₃ ^o	- 401,727.1 ₃	3.17E+08	1.87E+08 ^c
146.4069	335,112.2 ₂ ^o	- 403,415.0 ₂	6.11E+08	5.01E+08 ^c
147.5817	335,655.9 ₃ ^o	- 403,415.0 ₂	3.14E+09	1.87E+09 ^c
147.7002	380,434.8 ₂ ^o	- 448,139.5 ₂	1.67E+08	2.47E+09 ^c
149.9543	320,195.9 ₃ ^o	- 386,882.9 ₄	4.97E+09	5.97E+09 ^c
150.3041	335,655.9 ₃ ^o	- 402,187.7 ₂	5.28E+08	3.03E+09 ^c
151.3519	335,655.9 ₃ ^o	- 401,727.1 ₃	1.56E+09	2.68E+09 ^c
2759.3907	498,297.0 ₃ ^o	- 501,920.0 ₄ ^o	1.80E+03	7.94E+04 ^c
2997.7729	498,742.0 ₂ ^o	- 502,076.9 ₃ ^o	5.25E+03	1.14E+05 ^c
7889.2632	498,297.0 ₃ ^o	- 499,564.2 ₄ ^o	2.69E+03	4.39E+03 ^c
10,434.4792	513,177.0 ₃ ^o	- 514,135.1 ₂ ^o	6.45E+04	2.10E+04 ^c

a: Ritz wavelengths calculated employing the experimental energy level values from [50] [51]. Transitions are given by values (in cm⁻¹) of involved energy levels where subscripts denote their J-values. b: MCDHF values from [38]. pE + q = p.10^q. c: HFR values from [38]. d: Values from Newton method taken in [37].

4. Conclusions

We Critically evaluated available dipole-transition rates in Xe⁹⁺, Xe¹⁰⁺, Lu³⁺, Hf⁴⁺ and Ta⁵⁺ with respect to our recent results obtained through large-scale calculations using two independent theoretical methods, *i.e.* the semi-empirical Hartree-Fock with relativistic corrections method (HFR) and the *ab initio* multiconfiguration Dirac-Hartree-Fock method (MCDHF). The adopted data would allow plasma physicists to diagnose and model fusion plasmas in tokamaks where xenon, lutetium, hafnium and tantalum could be used.

In literature, transition probabilities and oscillator strengths of the studied

ions are all theoretical, so this work is a call for additional efforts to produce experimental data in order to refine theory. Producing these ions in the laboratory for their investigations is a challenging task.

It is well known that under conditions that prevail in many astrophysical and low-density laboratory tokamak plasmas, the collisional de-excitation of metastable states is rather slow, leading to the buildup of a population of metastable levels [52]. In this context, forbidden lines resulting from electric quadrupole (E2) and magnetic dipole (M1) transitions increase in intensity and can be used to deduce information about plasma temperature and dynamics. Therefore, we intend to extend our calculations to E2 and M1 transitions in Lu³⁺, Hf⁴⁺ and Ta⁵⁺.

Acknowledgements

Our own work, discussed in the framework of this review, was carried out in collaboration with P. Quinet and P. Palmeri (Atomic Physics and Astrophysics, Mons University, Belgium), and E. Bokamba Motoumba (Marien Ngouabi University, Congo). I would like to thank them very much. The Author is a Senior Lecturer at Marien Ngouabi University of Congo whose financial support is gratefully acknowledged.

Conflicts of Interest

The author declares no conflicts of interest regarding the publication of this paper.

References

- [1] Milora, S.C., Houlberg, W.A., Lengyel, W.A. and Mertens, V. (1995) Pellet Fuelling. *Nuclear Fusion*, **35**, 657-754. <https://doi.org/10.1088/0029-5515/35/6/I04>
- [2] Reznichenko, P.V., Vinyar, I.V. and Kuteev, B.V. (2000) An Injector of Xenon Macroscopic Pellets for Quenching the Fusion Reaction in a Tokamak. *Technical Physics*, **45**, 174-178. <https://doi.org/10.1134/1.1259592>
- [3] Beiersdorfer, P. (2015) Highly Charged Ions in Magnetic Fusion Plasmas: Research Opportunities and Diagnostic Necessities. *Journal of Physics B: Atomic, Molecular and Optical Physics*, **48**, Article ID: 144017. <https://doi.org/10.1088/0953-4075/48/14/144017>
- [4] Almandos, J.R. and Raineri, M. (2017) Spectral Analysis of Moderately Charged Rare-Gas Atoms. *Atoms*, **5**, Article No. 12. <https://doi.org/10.3390/atoms5010012>
- [5] Duchowicz, R., Schinca, D. and Gallardo, M. (1994) New Analysis for the Assignment of UV-Visible Ionic Xe Laser Lines. *IEEE Journal of Quantum Electronics*, **30**, 155-159. <https://doi.org/10.1109/3.272074>
<https://ieeexplore.ieee.org/document/272074>
- [6] Gallardo, M., Raineri, M., Reyna Almandos, J.G., Sobral, H. and Callegari, F. (1999) Revised and Extended Analysis in Four Times Ionized Xenon Xe V. *Journal of Quantitative Spectroscopy and Radiative Transfer*, **61**, 319-327. [https://doi.org/10.1016/S0022-4073\(97\)00237-9](https://doi.org/10.1016/S0022-4073(97)00237-9)
- [7] Sobral, H., Schinca, D., Gallardo, M. and Duchowicz, R. (1999) Time Dependent

- Study of a Multi-Ionic Xenon Plasma. *Journal of Applied Physics*, **85**, 69-73. <https://doi.org/10.1063/1.369422>
- [8] Sobral, H., Schinca, D., Gallardo, M. and Duchowicz, R. (1999) Excitation Mechanisms and Characterization of a Multi-Ionic Xenon Laser. *IEEE Journal of Quantum Electronics*, **35**, 1308-1313. <https://doi.org/10.1109/3.784590>
<https://ieeexplore.ieee.org/document/784590>
- [9] Rainieri, M., Lagorio, C., Padilla, S., Gallardo, M. and Reyna Almandos, J. (2008) Weighted Oscillator Strengths for the Xe IV Spectrum. *Atomic Data and Nuclear Data Tables*, **94**, 140-159. <https://doi.org/10.1016/j.adt.2007.10.001>
- [10] Reyna Almandos, J., Bredice, F., Rainieri, M. and Gallardo, M. (2009) Spectral Analysis of Ionized Noble Gases and Implications for Astronomy and Laser Studies. *Physica Scripta*, **2009**, Article ID: 014018.
<https://doi.org/10.1088/0031-8949/2009/T134/014018>
- [11] Gallardo, M., Rainieri, M., Reyna Almandos, J. and Biémont, E. (2011) New Energy Levels, Calculated Lifetimes and Transition Probabilities in Xe IX. *Journal of Physics B: Atomic, Molecular and Optical Physics*, **44**, Article ID: 045001.
<https://doi.org/10.1088/0953-4075/44/4/045001>
- [12] Biémont, E., Quinet, P. and Zeippen, C.J. (2005) Transition Probabilities in Xe V. *Physica Scripta*, **71**, 163-169. <https://doi.org/10.1238/Physica.Regular.071a00163>
- [13] Biémont, E., Buchard, V., Garnir, H.P., Lefèuvre, P.H. and Quinet, P. (2005) Radiative Lifetime and Oscillator Strength Determinations in Xe VI. *The European Physical Journal D—Atomic, Molecular, Optical and Plasma Physics*, **33**, 181-191.
<https://doi.org/10.1140/epjd/e2005-00059-y>
- [14] Biémont, E., Clar, M., Fivet, V., Garnir, H.P., Palmeri, P., Quinet, P. and Rostohar, D. (2007) Lifetime and Transition Probability Determination in Xenon Ions. *The European Physical Journal D—Atomic, Molecular, Optical and Plasma Physics*, **44**, 23-33. <https://doi.org/10.1140/epjd/e2007-00161-2>
- [15] Garnir, H.P., Enzonga Yoca, S., Quinet, P. and Biémont, E. (2009) Lifetime and Transition Probability Determination in Xe IX. *Journal of Quantitative Spectroscopy and Radiative Transfer*, **110**, 284-292. <https://doi.org/10.1016/j.jqsrt.2008.11.007>
- [16] Quinet, P., Palmeri, P., Biémont, E., McCurdy, M.M., Rieger, G. and Pinnington, E.H. (1999) Experimental and Theoretical Radiative Lifetimes, Branching Fractions and Oscillator Strengths in Lu II. *Monthly Notices of the Royal Astronomical Society*, **307**, 934-940. <https://doi.org/10.1046/j.1365-8711.1999.02689.x>
- [17] Grant, I.P. and McKenzie, B.J. (1980) The Transverse Electron-Electron Interaction in Atomic Structure Calculations. *Journal of Physics B: Atomic and Molecular Physics*, **13**, Article No. 2671. <https://doi.org/10.1088/0022-3700/13/14/007>
- [18] Grant, I.P., McKenzie, B.J., Norrington, P.H., Mayers, D.F. and Pyper, N.C. (1980) An Atomic Multiconfigurational Dirac-Fock Package. *Computer Physics Communications*, **21**, 207-231. [https://doi.org/10.1016/0010-4655\(80\)90041-7](https://doi.org/10.1016/0010-4655(80)90041-7)
- [19] McKenzie, B.J., Grant, I.P. and Norrington, P.H. (1980) A Program to Calculate Transverse Breit and QED Corrections to Energy Levels in a Multiconfiguration Dirac-Fock Environment. *Computer Physics Communications*, **21**, 233-246.
[https://doi.org/10.1016/0010-4655\(80\)90042-9](https://doi.org/10.1016/0010-4655(80)90042-9)
- [20] Dyall, K.G., Grant, I.P., Johnson, C.T., Parpia, F.A. and Plummer, E.P. (1989) GRASP: A General-Purpose Relativistic Atomic Structure Program. *Computer Physics Communications*, **55**, 425-456. [https://doi.org/10.1016/0010-4655\(89\)90136-7](https://doi.org/10.1016/0010-4655(89)90136-7)
- [21] Träbert, E. (2008) Beam-Foil Spectroscopy-Quo Vadis? *Physica Scripta*, **78**, Article ID: 038103. <https://doi.org/10.1088/0031-8949/78/03/038103>

- [22] Saloman, E.B. (1983) Energy Levels and Observed Spectral Lines of Xenon, Xe I through Xe LIV. *Journal of Physical and Chemical Reference Data*, **33**, 765-921. <https://doi.org/10.1063/1.1649348>
- [23] Kaufman, V., Sugar, J. and Tech, J.L. (1983) Analysis of the $4d^9-4d^85p$ Transitions in Nine-Times Ionized Xenon (Xe X). *Journal of the Optical Society of America*, **73**, 691-693. <https://doi.org/10.1364/JOSA.73.000691>
- [24] Churilov, S.S. and Joshi, Y.N. (2002) Analysis of the $4p^64d^84f$ and $4p^54d^{10}$ Configurations of Xe X and Some Highly Excited Levels of Xe VIII and Xe IX Ions. *Physica Scripta*, **65**, 40-54. <https://doi.org/10.1238/Physica.Regular.065a00040>
- [25] Churilov, S., Joshi, Y.N. and Reader, J. (2003) High-Resolution Spectrum of Xenon ions at 13.4 nm. *Optics Letters*, **28**, 1478-1480. <https://doi.org/10.1364/OL.28.001478>
- [26] Fahy, K., Sokell, E., O'Sullivan, G., Aguilar, A., Pomeroy, J.M., Tan, J.N. and Gillaspy, J.D. (2007) Extreme-Ultraviolet Spectroscopy of Highly Charged Xenon Ions Created Using an Electron-Beam Ion Trap. *Physical Review A*, **75**, Article ID: 032520. <https://doi.org/10.1103/PhysRevA.75.032520>
- [27] Bokamba Motoumba, E., Enzonga Yoca, S., Palmeri, P. and Quinet, P. (2019) Relativistic Hartree-Fock and Dirac-Fock Atomic Structure and Radiative Parameter Calculations in Nine-Times Ionized Xenon (Xe X). *Journal of Quantitative Spectroscopy and Radiative Transfer*, **227**, 130-135. <https://doi.org/10.1016/j.jqsrt.2019.01.028>
- [28] Churilov, S.S., Joshi, Y.N., Reader, J. and Kildiyarova, R.R. (2004) $4p^64d^8 - (4d^75p + 4d^74f + 4p^54d^9)$ Transitions in Xe XI. *Physica Scripta*, **70**, 126-138. <https://doi.org/10.1088/0031-8949/70/2-3/009>
- [29] Shen, Y., Gao, C. and Zeng, J. (2009) Electron Impact Collision Strengths and Transition Rates for Extreme Ultraviolet Emission from Xe^{10+} . *Atomic Data and Nuclear Data Tables*, **95**, 1-53. <https://doi.org/10.1016/j.adt.2008.07.001>
- [30] Bokamba Motoumba, E., Enzonga Yoca, S., Quinet, P. and Palmeri, P. (2019) *Ab Initio* MCDHF/RCI and Semi-Empirical HFR Calculations of Transition Probabilities and Oscillator Strengths in Xe XI. *Journal of Quantitative Spectroscopy and Radiative Transfer*, **235**, 217-231. <https://doi.org/10.1016/j.jqsrt.2019.07.006>
- [31] Pillon, M., Angelone, M. and Forrest, R.A. (2004) Measurements of Fusion-Induced Decay Heat in Materials and Comparison with Code Predictions. *Radiation Physics and Chemistry*, **71**, 895-896. <https://doi.org/10.1016/j.radphyschem.2004.04.119>
- [32] Ryabtsev, A.N., Ya Kononov, E., Kildiyarova, R.R., Tchang-Brillet, W.-Ü.L., Wyart, J.-F., Champion, N. and Blaess, C. (2014) Spectra of the W VIII Isoelectronic Sequence: I. Hf VI. *Physica Scripta*, **89**, Article ID: 115402. <https://doi.org/10.1088/0031-8949/89/11/115402>
- [33] Ryabtsev, A.N., Ya Kononov, E., Kildiyarova, R.R., Tchang-Brillet, W.-Ü.L., Wyart, J.-F., Champion, N. and Blaess, C. (2014) Spectra of the W VIII Isoelectronic Sequence: II. Ta VII. *Physica Scripta*, **89**, Article ID: 125403. <https://doi.org/10.1088/0031-8949/89/12/125403>
- [34] Linsmeier, Ch., Rieth, M., Aktaa, J., Chikada, T., Hoffmann, A., Hoffmann, J., et al. (2017) Development of Advanced High Heat Flux and Plasma-Facing Materials. *Nuclear Fusion*, **57**, Article ID: 092007. <https://doi.org/10.1088/1741-4326/aa6f71>
- [35] Gilbert, M.R. and Sublet, J.-C. (2011) Neutron-Induced Transmutation Effects in W and W-Alloys in a Fusion Environment. *Nuclear Fusion*, **51**, Article ID: 043005. <https://doi.org/10.1088/0029-5515/51/4/043005>
- [36] Anisimova, G.P., Loginov, A.V. and Tuchkin, V.I. (2001) Probabilities of Electric

Dipole Transitions in the Spectra of Ions of the Erbium Isoelectronic Sequence. *Optics and Spectroscopy*, **90**, 315-320. <https://doi.org/10.1134/1.1358433>

- [37] Loginov, A.V. and Tuchkin, V.I. (2001) Radiative Constants in the Spectra of Ions of the Erbium Isoelectronic Sequence. *Optics and Spectroscopy*, **90**, 631-638. <https://doi.org/10.1134/1.1374646>
- [38] Bokamba Motoumba, E., Enzonga Yoca, S., Quinet, P. and Palmeri, P. (2020) Calculations of Transition Rates in Erbium-Like Ions Lu IV, Hf V and Ta VI Using the *Ab Initio* MCDHF-RCI and Semi-Empirical HFR Methods. *Atomic Data and Nuclear Data Tables*, **133-134**, Article ID: 101340. <https://doi.org/10.1016/j.adt.2020.101340>
- [39] Jonsson, P., He, X., Froese Fischer, C. and Grant, I.P. (2007) The Grasp2K Relativistic Atomic Structure Package. *Computer Physics Communications*, **177**, 597-622. <https://doi.org/10.1016/j.cpc.2007.06.002>
- [40] Froese Fischer, C., Gaigalas, G., Jönsson, P., Bieroń, J. and Grant, I.P. (2019) GRASP2018—A Fortran 95 Version of the General Relativistic Atomic Structure Package. *Computer Physics Communications*, **237**, 184-187. <https://doi.org/10.1016/j.cpc.2018.10.032>
- [41] Froese Fischer, C., Godefroid, M.R., Brage, T., Jönsson, P. and Gaigalas, G. (2016) Advanced Multiconfiguration Methods for Complex Atoms: I. Energies and Wave Functions. *Journal of Physics B: Atomic, Molecular and Optical Physics*, **49**, Article ID: 182004. <https://doi.org/10.1088/0953-4075/49/18/182004>
- [42] Carette, T., Drag, C., Scharf, O., Blondel, C., Delsart, C., Froese Fischer, C. and Godefroid, M.R. (2010) Isotope Shift in the Sulfur Electron Affinity: Observation and Theory. *Physical Review A*, **81**, Article ID: 042522. <https://doi.org/10.1103/PhysRevA.81.042522>
- [43] Zhang, W., Palmeri, P., Quinet, P. and Biemont, E. (2013) Transition Probabilities in Te II and Te III Spectra. *Astronomy & Astrophysics*, **551**, Article No. A136. <https://doi.org/10.1051/0004-6361/201220918>
- [44] Cowan, R.D. (1981) The Theory of Atomic Structure and Spectra. University of California Press, Berkeley. <https://doi.org/10.1525/9780520906150>
- [45] Slater, J.C. (1960) Quantum Theory of Atomic Structure. Vol. I-II, McGraw-Hill Book Company, New York.
- [46] Gu, M.F. (2008) The Flexible Atomic Code. *Canadian Journal of Physics*, **86**, 675-689. <https://doi.org/10.1139/p07-197>
- [47] Sugar, J. and Kaufman, V. (1972) Fourth Spectrum of Lutetium. *Journal of the Optical Society of America*, **62**, 562-570. <https://doi.org/10.1364/JOSA.62.000562>
- [48] Sugar, J. and Kaufman, V. (1974) Spectra and Energy Levels of Three- and Four-Times Ionized Hafnium (Hf iv and Hf v). *Journal of the Optical Society of America*, **64**, 1656-1664. <https://doi.org/10.1364/JOSA.64.001656>
- [49] Kaufman, V. and Sugar, J. (1975) Spectrum and Energy Levels of Five-Times Ionized Tantalum (Ta vi). *Journal of the Optical Society of America*, **65**, 302-309. <https://doi.org/10.1364/JOSA.65.000302>
- [50] Sugar, J. and Kaufman, V. (1975) Seventh Spectrum of Tungsten (W vii); Resonance Lines of Hf v. *Physical Review A*, **12**, 994-1012. <https://doi.org/10.1103/PhysRevA.12.994>
- [51] Wyart, J.-F., Kaufman, V. and Sugar, J. (1981) The $4f^{13}5f$ Configuration in the Isoelectronic Sequence of Yb III. *Physica Scripta*, **23**, 1069-1078. <https://doi.org/10.1088/0031-8949/23/6/008>

- [52] Charro, E., Curiel, Z. and Martin, I. (2002) Atomic Data for M1 and E2 Emission Lines in the Potassium Isoelectronic Sequence. *Astronomy & Astrophysics*, **387**, 1146-1152. <https://doi.org/10.1051/0004-6361:20020288>